

EM 343-494

Voyager

**Voyager Spacecraft 31
Canopus Star Tracker S/N 205
Failure Investigation**

Morris M. Birnbaum
Phil M. Salomon
Ray Uematsu

24 September 1980

National Aeronautics and
Space Administration

Jet Propulsion Laboratory
California Institute of Technology
Pasadena, California

SUMMARY

This report describes the failure investigation of the Canopus Star Tracker (CST), S/N 205, on Voyager Spacecraft 31. A detailed description of the failure models investigated, and their evolution to the presently believed failure mode, is described.

The most probable cause of the Voyager Spacecraft 31 Canopus Star Tracker (CST) cone angle anomaly is failure of a SDT 5553 transistor which drives the cone angle deflection plates. The failure is caused by either a base-emitter or a collector-emitter leakage in the transistor.

Using a spare CST, the presumed leakage was modeled, first with a resistor strapped between the collector and emitter of the suspect transistor, and then between the base and ground. Excellent duplication of the anomalies observed in the Spacecraft Star Tracker were obtained in both cases.

The most probable cause of the leakage path of the SDT 5553 transistor is the failure of the Delrin sleeves placed on the transistor leads to insulate them as they come through a tungsten box in which the transistors are placed for radiation shielding. Information received about Delrin from DuPont, the manufacturer, and Naval Research Laboratory personnel in Washington, D.C., indicates that Delrin decomposes when exposed to radiation. It is very likely that two or more Delrin insulating sleeves have decomposed, resulting in a high resistance (over 500,000 ohms) leakage path between the SDT 5553 leads, causing the transistor to appear to be almost saturated all of the time.

An electrostatic discharge analysis was performed on the tungsten spot shield box in which the SDT 5553 transistors were placed. The tungsten box was epoxyed to the printed circuit board containing the cone angle deflection circuitry, and was not grounded. The electrostatic discharge analysis showed that, even though inside the CST housing, the tungsten box could charge up to 350 volts or more. It is highly probable that a discharge occurred from the tungsten box through a Delrin sleeve containing microvoids or scratches, and decomposing, producing HF (Hydrofluoric acid). This presumed discharge could carbonize a path through the defective Delrin, resulting in a stable high resistance path, causing the leak associated with the SDT 5553 transistor.

It is recommended that Delrin not be used as insulating sleeving in future Space applications. It is also recommended that all metal shielding boxes or metal masses on circuit boards be grounded, even though they are inside equipment housings. If large radiation fields are encountered, these metal masses can become charged. If not grounded, a discharge through defective insulators can occur, thus causing a failure in an otherwise marginal, but still functional system.

CONTENTS

1.	BASIC CANOPUS STAR TRACKER DESIGN	1-1
1.1	GENERAL DESCRIPTION.	1-1
1.2	DATA NUMBERS	1-4
2.	HISTORY OF CST NO. 205 SINCE LAUNCH	2-1
2.1	CST CONE ANGLE/INTENSITY HISTORY	2-1
2.2	INITIAL FAILURE DIAGNOSIS.	2-2
2.3	INVESTIGATION PROCEDURE.	2-2
3.	INITIAL FAILURE INVESTIGATION	3-1
3.1	CONE ANGLE SELECTION SYSTEM.	3-1
3.2	CONE ANGLE SELECTION SYSTEM IN HYBIC PROCESSOR	3-1
3.3	DEDICATED CIRCUITRY FOR CONE ANGLE SWITCHING	3-3
3.4	LOGIC STATE "0" FAILURE MODES OF "COMMAND B" DEDICATED CIRCUITRY.	3-5
3.4.1	"Command B" Storage Register.	3-5
3.4.2	"Command B" LM124 Operational Amplifier	3-6
3.4.3	"Command B" LM 103-3.0 Zener Diode.	3-6
3.4.4	"Command B" 2N2222A Transistor Switch	3-7
3.5	WORKAROUND	3-8
3.6	RECOMMENDATION	3-10
3.7	CST S/N 205 CONE ANGLE MEASUREMENTS.	3-14
3.8	CONE ANGLE MEASUREMENT CONCLUSIONS	3-14

4.	CONE ANGLE DEFLECTION SYSTEM INVESTIGATION.	4-1
4.1	LM108AH REFERENCE AMPLIFIER U1	4-1
4.2	CONE DEFLECTION TRANSISTOR, SDT 5553 (Q5).	4-1
4.3	SIMULATION OF SDT 5553 (Q5) FAILURE MODE	4-1
4.4	ZENER DIODE, UZ8770 (CR5).	4-4
4.5	SDT 5553 TRANSISTOR DESIGN AND USE IN CST.	4-4
4.6	CAUSES OF SDT 5553 FAILURE	4-5
5.	DELFIN AF INVESTIGATION	5-1
5.1	DELFIN AF SLEEVE DESIGN.	5-1
5.2	DELFIN AF DESCRIPTION.	5-1
5.3	ELECTROSTATIC CHARGING OF DELFIN AF SLEEVES.	5-3
5.4	PROPOSED SCENARIO OF EVENTS CAUSING FAILURE.	5-4
6.	CST 205 INTENSITY VARIATION INVESTIGATION	6-1
6.1	INTENSITY HISTORY AFTER ANOMALY DISCOVERY	6-1
6.2	INTENSITY PROBLEM SIMULATION	6-2
6.3	DEFOCUSING MECHANISM	6-3
6.4	DEFOCUSING EFFECT ON DIM STARS	6-5
6.5	DEFOCUSING EFFECT ON ROLL ERROR SIGNAL	6-7
6.6	CONCLUSION	6-7
APPENDIX A	A-2
NOTE 1	A-9
NOTE 2	A-12
NOTE 3	A-14
NOTE 4	A-14
NOTE 5	A-15
REFERENCES FOR APPENDIX	A-17

Figures

1.	Canopus Star Tracker Schematic	1-2
2.	Canopus Star Tracker Cone Angle Fields of View	1-3
3.	Cone Angle Versus DN	1-5
4.	Star Intensity Versus DN	1-6
5.	Canopus Star Tracker Cone Angle Generation Circuitry	3-2
6.	Hybrid Buffer Interface Circuit (HYBIC).	3-4
7.	Hardware Review/Certification Requirement Form	3-9
8.	Cone Angles Achieved with Leakage Model Star Scanner	3-13
9.	LM 108AH Schematic	4-2
10.	Cone Angles Commanded Versus DN Achieved for Q5 Collector-Emitter Leakage.	4-3
11.	Tungsten Box for SDT 5553 Transistors	4-6
12.	Delrin AF Sleeve Design.	5-2
13.	Electron Beam Defocusing	6-4
14.	CST Intensity Readout for Dimmer Stars	6-6
15.	Roll Error Noise in Cone Angle C2 for Various Star Intensities (1.0 to 0.122 x Canopus)	6-8
16.	Roll Error Noise in Cone Angle C2 for Various Star Intensities (0.06 to 0.027 x Canopus)	6-9
17.	Roll Error Noise in Cone Angle C8 for Various Star Intensities (1.0 to 0.122 x Canopus)	6-10
18.	Roll Error Noise in Cone Angle C8 for Various Star Intensities (0.06 to 0.227 x Canopus)	6-11
A-1.	Schematic of the Tungsten Spot Shield	A-3
A-2.	Equivalent Circuit of Figure A-1	A-3
A-3.	SDT 5553 Transistors Assembled in Container	A-10
A-4.	Tungsten Spot Shield Box	A-11
A-5.	Delrin Sleeve.	A-13
A-6.	Range Curve	A-16

Tables

1.	CST Cone Angle/Intensity History Up to Anomaly Discovery	2-1
2.	Cone Angle Generation Logic.	3-3
3.	Dedicated Circuitry Table.	3-5
4.	Cone Angle Versus "Command B" Line Input Voltage (Zener Diode Shorted; Cone Angle 3 Command On Pins C, D, E)	3-7
5.	Cone Angle Achieved with Leaky Q2.	3-10
6.	Voyager Spacecraft 31-CST Cone Angle-Intensity History on Day 80-233 (20 August 1980).	3-14
7.	Voyager Spacecraft 31-CST Cone Angle Intensity History on Days 80-235 Through 80-242	6-1
8.	CST, S/N 203, Intensity Readings with Defective Cone Angle Circuit.	6-2
9.	Voltage on Cone Angle Deflection Plates.	6-5
A-1.	Voyager 1 Jupiter Encounter Peak Electron Flux Spectra	A-4
A-2.	Properties of Delrin	A-5
A-3.	Results of Circuit Analysis.	A-7

SECTION 1

BASIC CANOPUS STAR TRACKER DESIGN

1.1 GENERAL DESCRIPTION

The Canopus Star Tracker (CST) employs an image dissector tube as its light sensor. The CST optical system focuses a 36 degree by 10 degree field of view on the tube photocathode. The image dissector tube uses an electrostatic deflection system, allowing any discrete area of the photocathode to be examined for the presence of a light signal through the one degree by twelve degree slit aperture at the electro-optical focal plane of the tube. A schematic of the deflection system is shown in Figure 1, Canopus Star Tracker Schematic.

The 36 degree dimension of the field of view is in the direction of the "Z" axis of the Spacecraft. The ten degree dimension of the field is along the "roll" direction of the Spacecraft, when the Spacecraft rotates about the Z axis. The division of the 36 by 10 degree field of view into five cone angles is shown in Figure 2, Canopus Star Tracker Cone Angle Fields of View.

By putting a sinusoidal dithering voltage on the "roll" plates of the image dissector tube deflection system, the area around the basic five cone angles can be inspected for light (Canopus, or some other guide star). If a star is sensed, roll error signals are generated such that the Spacecraft is rotated about its Z axis until the star is at the "roll" center line of the field of view, the centerline going in the $\pm Z$ axis direction. The CST is a one axis nulling system, meaning it only generates error signals along its roll axis when the light source focused on the photocathode is not at the "roll" centerline of the field of view. No cone error signal is generated, since the cone deflection plates have no dithering voltage on them. Therefore, as long as the light source or star is focused somewhere in the area inspected by the one-by-twelve degree rectangular slit, only roll error information is generated.

The purpose of using an image dissector tube as the light sensing element of the Canopus Star Tracker is to obtain an extremely high signal-to-noise ratio. By limiting the area of the photocathode contributing noise photoelectrons to just the area deflected into the dissector aperture slit, the complete signal, if present, is sensed, but only the noise contribution from the desired deflected area, rather than from the total photocathode. Also, by dithering the deflected area on either side of the light signal, (usually Canopus), most of the time the signal is in the deflected area, so a maximum of signal energy is being sensed. Also, very narrow bandpass filters, centered about the dither frequency can be used, to discriminate against wideband noise. The result of scanning only a small photocathode area, sensing star energy for most of the dither cycle, and using a narrow band-pass filter, is a very high signal-to-noise ratio, unachievable by almost any other device or technique.

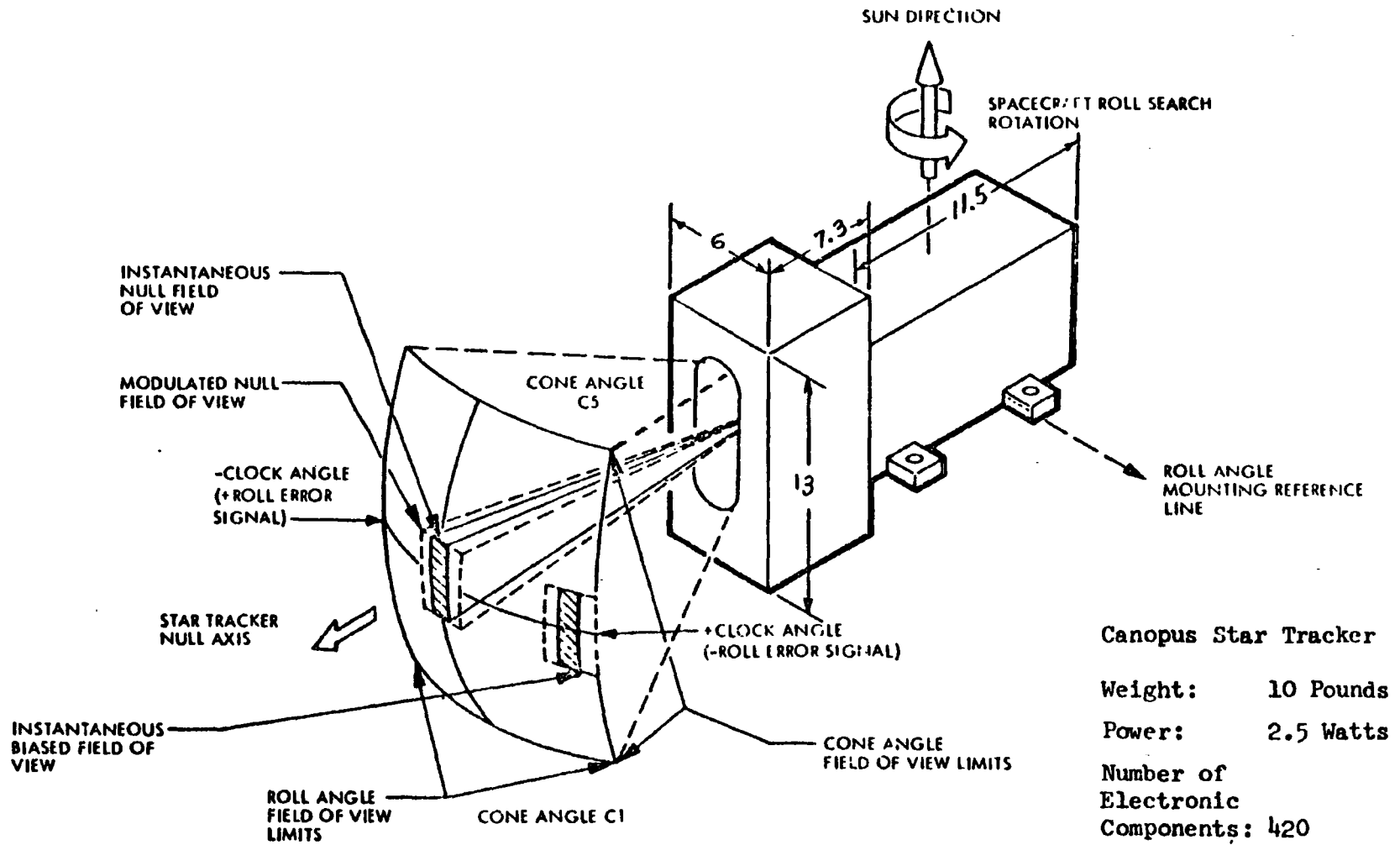
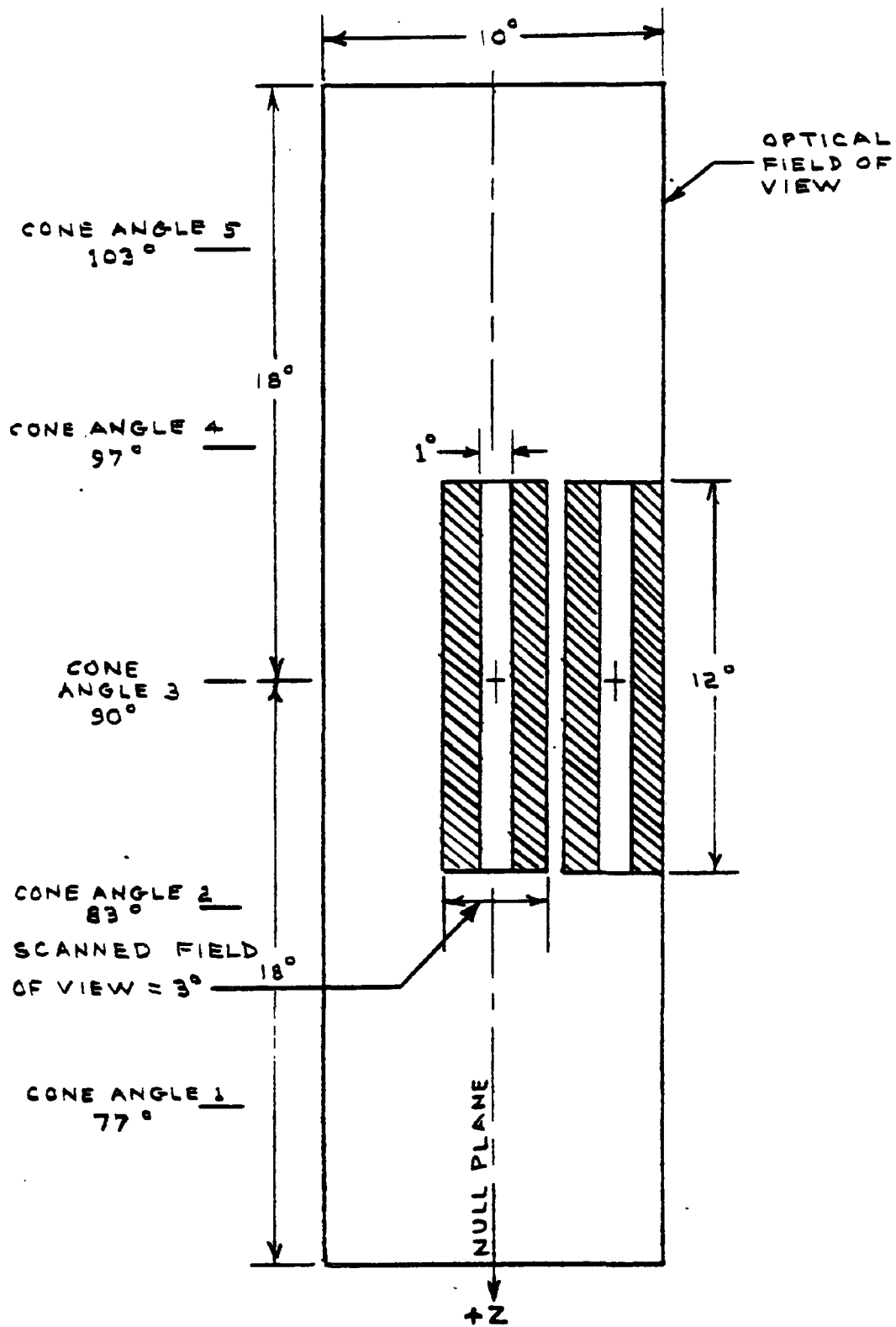


Figure 1. Canopus Star Tracker Schematic



**CANOPUS STAR TRACKER
CONE ANGLE FIELDS OF VIEW**

Figure 2. Canopus Star Tracker Cone Angle Fields of View

1.2 DATA NUMBERS

When incorporated into the Voyager Spacecraft, the operation of the CST is monitored by telemetering back to Earth various CST outputs such as:

- Roll error Signal
- Intensity of star signal being sensed
- Cone angle in which CST is operating
- CST temperature

The above outputs, each on its own channel, are telemetered in the form of a data number (DN), a digital number related to the analog voltage it represents. Since each CST output covers a unique voltage range, the DN-analog voltage relationship is different for each channel. The relationship between the CST analog output voltage representing the cone angle being scanned, and the DN telemetered is shown in Figure 3, Cone Angle Versus DN.

The relationship between the CST analog output voltage representing the intensity of the star signal being sensed and the DN telemetered is shown in Figure 4, Star Intensity Versus DN. By careful calibration on the ground, before Voyager was launched, and by recalibration during the Voyager trajectory, the DN for each channel is well known for the CST analog signal voltage it represents.

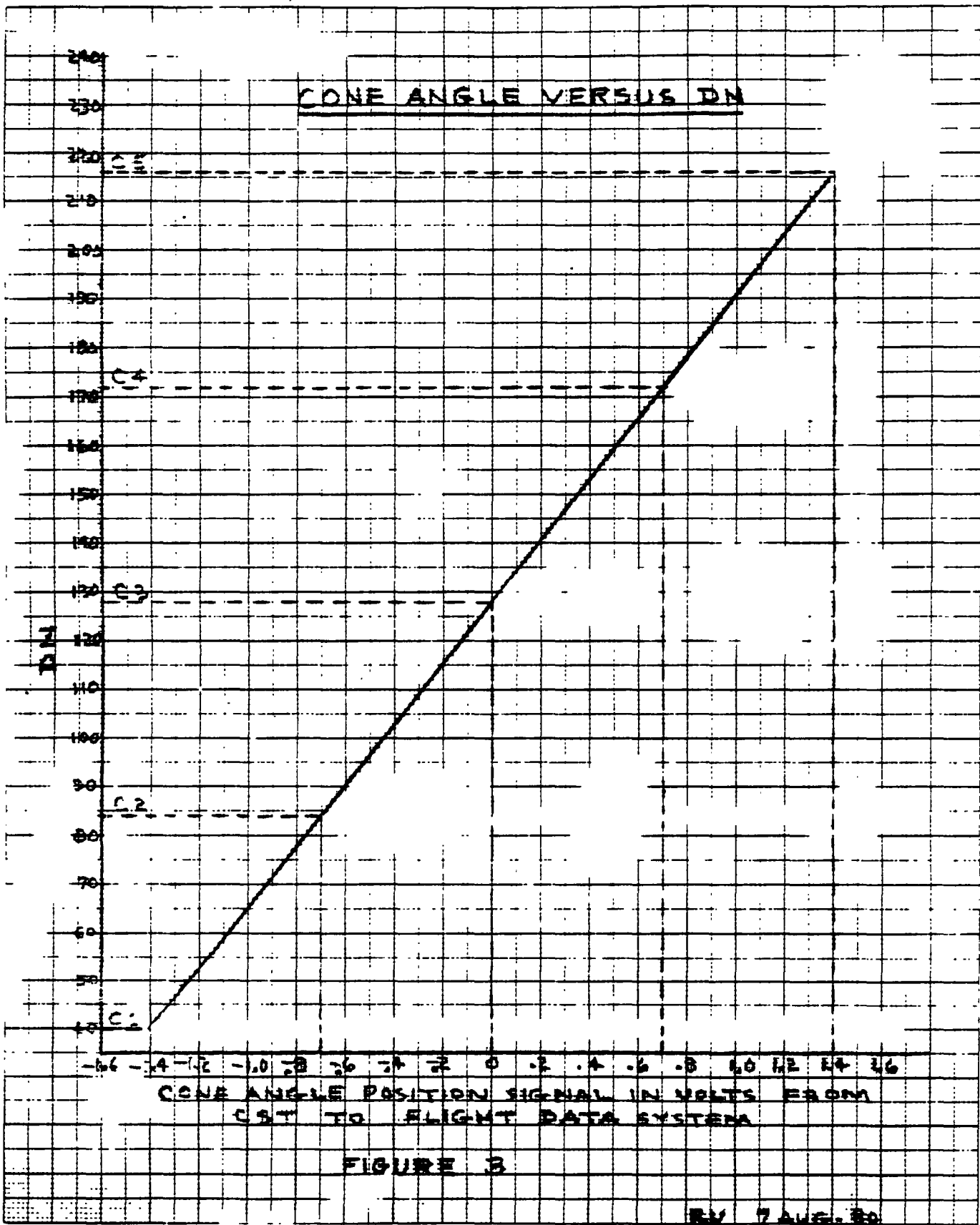


Figure 3. Cone Angle Versus DN

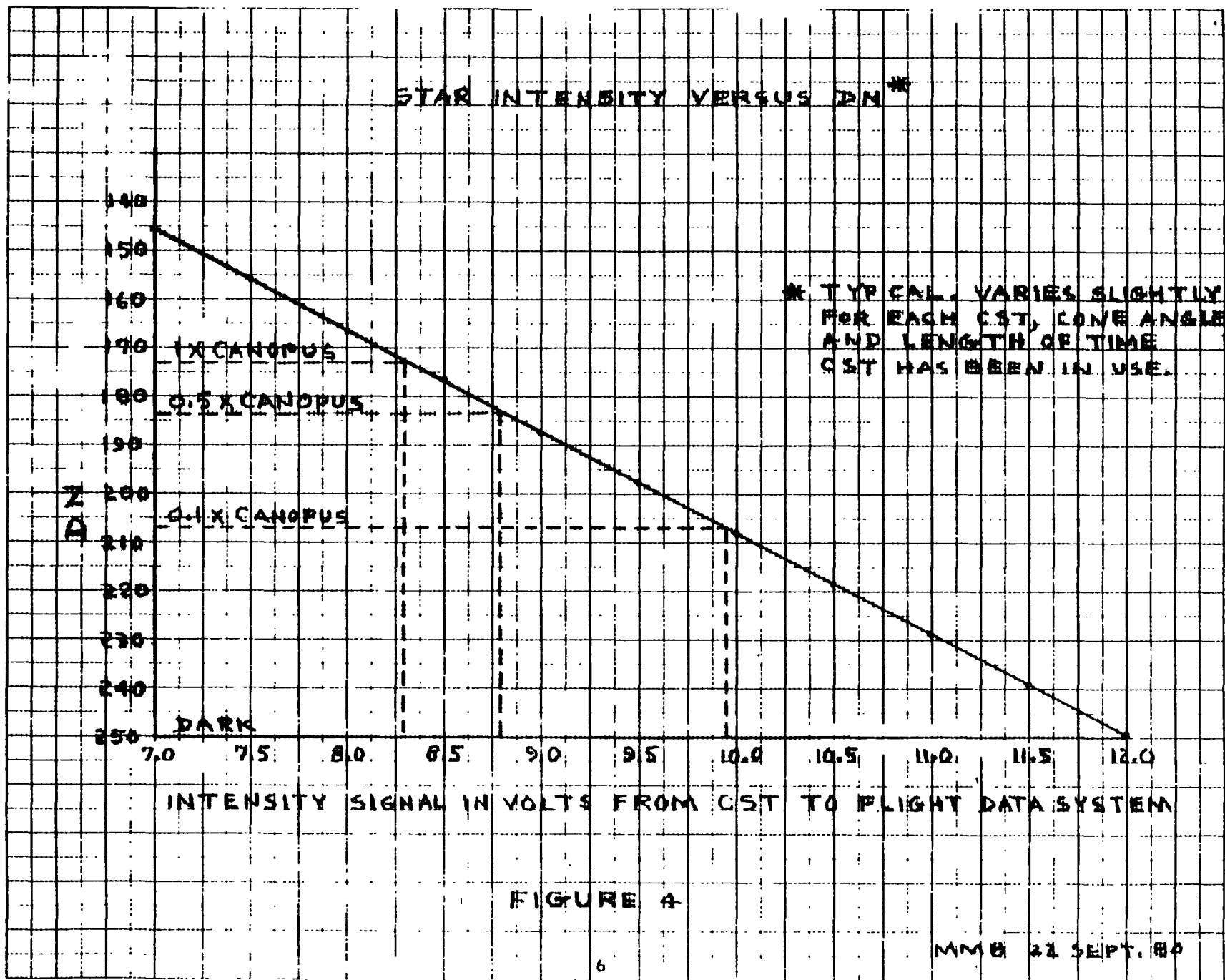


Figure 4. Star Intensity Versus DN

SECTION 2

HISTORY OF CST NO. 205 SINCE LAUNCH

2.1 CST CONE ANGLE/INTENSITY HISTORY

Since launch, Voyager Spacecraft 31 has been operated with its CST 205 switched to the cone angles shown and viewing the stars noted in Table 1 below:

Table 1. CST Cone Angle/Intensity History up to Anomaly Discovery

Date	Cone Angle Commanded	Cone Angle DN	Intensity DN	Star Being Tracked	Comments
77-248-77-280	C4	165.67	176.60	Canopus	Launch 5, Sept. 1977
77-280-77-303	C3	128.15	176.17	Canopus	
77-303-78-047	C2	84.70	176.71	Canopus	
78-047-79-064	C1	45.13	180.10	Canopus	Jupiter Encounter
79-064-79-096	C2	79.36	201.49	Arcturus	
79-096-79-182	C1	45.14	183.42	Canopus	
79-182-80-091	C2	81.48	183.97	Canopus	
80-091-80-095	C1	45.06	218.76	Miaplacidus	
80-095-80-121	C2	82.24	184.49	Canopus	
80-121	C4	94.43	--	Vega	Anomaly! (Roll Turn Test). Should Read DN 165-166
80-121-80-204	C2	82.23	185.04	Canopus	
80-204-80-205	C1	45.14	226.81	Alhena	
80-205 80-230	C3	87.62	186.01	Canopus	Anomaly! Should Read DN 128

2.2 INITIAL FAILURE DIAGNOSIS

Until Jupiter encounter on 5 March 1979, the CST operated properly in cone angles C4, C3, C2, and C1. Encounter occurred in C1. The following day the CST was switched to C2 to track Arcturus since Canopus was occulted by Jupiter. In April 1980, the CST was switched to C1 to track Miaplacidus, and then back to C2 and Canopus. On 30 April 1980, the CST was commanded to go to cone angle C4 for a roll turn test, sense Vega, and then return to C2 and Canopus. Though not noticed at the time, later inspection of the telemetry showed that the CST never went to cone angle C4, but moved to a cone angle between C2 and C3. The CST, after being commanded to go to C2, remained there until 22 July 1980, when it was commanded to move to C1. On the 23 July 1980, the CST was commanded to move to cone angle C3. The return telemetry showed that the CST had actually moved approximately to cone angle C2. This was verified by a Spacecraft test on 10 August 1980, by rotating the Spacecraft about an axis perpendicular to the Z axis so that Canopus moved up and down (constant clock angle) through the complete cone angle which the CST was actually at, and sensing when Canopus disappeared from the CST field of view. This test showed that the CST was really in cone angle C2, although the telemetry from the command registers showed that cone angle C3 was being inputted to the CST. Examining the above cone angle history, it was seen that (1) no anomalies in cone angle position occurred before Jupiter encounter; (2) two anomalies, one when commanded to move to C4, and one when commanded to move to C3, occurred since encounter; (3) no anomalies have occurred since Jupiter encounter when cone angle commands have been to move to C1 or C2.

2.3 INVESTIGATION PROCEDURE

In searching for the cause of the trouble, certain observations were made to be able to focus quickly on the possible problem area. These observations were:

- (1) Until Jupiter encounter, the CST operated properly in moving to cone angles C1, C2, C3, and C4.
- (2) After Jupiter encounter, the CST operated properly in moving to cone angles C1 and C2.
- (3) After Jupiter encounter, the CST has not operated properly in moving to cone angles C4 and C3.
- (4) Therefore, it seems likely that circuitry in the cone angle generating subsystems common to all of the angles is functioning properly.
- (5) Most probable area of malfunction is cone angle circuitry dedicated to cone angles 3 and 4 and not common to the other cone angles.
- (6) Circuitry dedicated to the individual cone angles (the switching circuitry determining the specific cone angle) is located in the Hybrid Buffer Interface Circuit (HYBIC) and in the CST cone angle command input stages. Therefore, these are the areas to examine first for failures which could cause the observed anomalies.

SECTION 3

INITIAL FAILURE INVESTIGATION

3.1 CONE ANGLE SELECTION SYSTEM

To choose one of the five cone angles, the CST has been designed with three cone angle "command" inputs, each one controlling a transistor switch. The circuitry schematic is shown in Figure 5, CST Cone angle Generation Circuitry. Logic levels, inputted on pins C, D, and E, either turn-on or keep off transistors Q1, Q2, and Q3. These transistors are connected to a resistor ladder network and, when turned on and in saturation, ground the 390K Ω resistor connected to their collectors. When turned off and essentially open, they allow a +5.5 volt level to occur at the 390K Ω resistors. Depending on which combination of the three switching transistors. Q1, Q2, and Q3 are in saturation or off, the voltage drop across the resistor ladder network composed of R24, R25, and R26 can be varied and cause a unique voltage to occur at R23, the + input of the differential operational amplifier, U1. Since there are three switching transistors, Q1, Q2, and Q3, and each transistor can assume two states, eight voltage levels at the input to U1 are possible. In the CST design, only five different combinations of Q1, Q2, and Q3 are used to give the five cone angles. These are shown in the Table 2, below.

Table 2. Cone Angle Generation Logic

Cone Angle	Logic Level Pin			TLM CST Cone Angle Pos'n Reading (volts)	DN (Typical)
	C	D	E		
C1	1	1	1	-1.46	40
C2	1	1	0	-0.75	84
C3	1	0	1	0	128
C4	1	0	0	+0.75	172
C5	0	1	1	+1.46	216
THE FOLLOWING COMBINATIONS ARE NOT USED					
C6	0	1	0	+1.68	---
C7	0	0	1	+1.68	---
C8	0	0	0	+1.68	---

Logic Level 0 = 0 \pm 0.5 VdcLogic Level 1 = 8.2 \pm 1.0 Vdc

C1 is towards +Z; C5 is towards -Z.

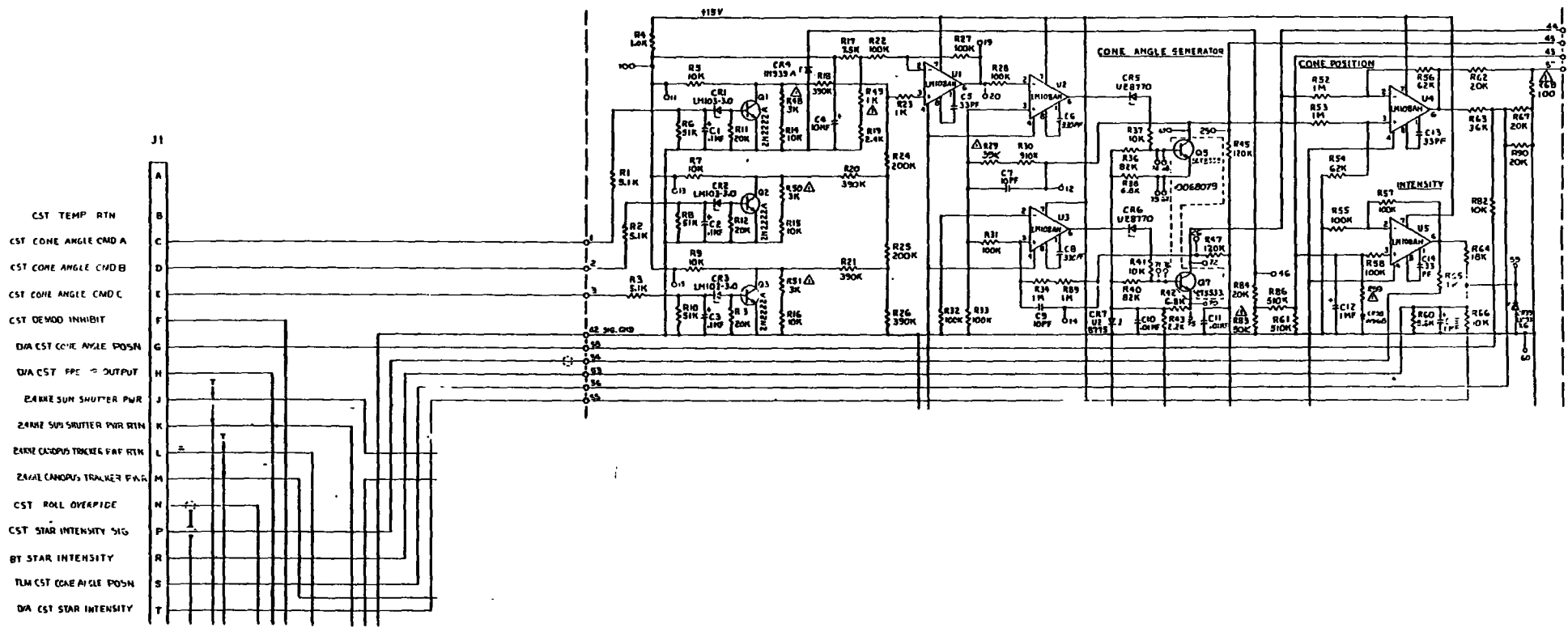


Figure 5. Canopus Star Tracker Cone Angle Generation Circuitry

3.2 CONE ANGLE SELECTION SYSTEM IN HYBIC PROCESSOR

The three "command" inputs to the CST transistor switches Q1, Q2, and Q3, come from the HYBIC. A schematic is shown in Figure 6, HYBIC. From the AACS Central Processing Unit, commands are serial-inputted into a shift register, U32 through U35. The logic levels are shifted across the shift register so that each individual shift register flip-flop holds a "1" or a "0" logic level. When a "load" pulse is received, the logic level of each shift register flip-flop is parallel-loaded in a storage register flip-flop (U21-U24) directly connected to a shift register flip-flop. The shift register can now receive other commands (logic levels) without disturbing the logic levels stored in the storage register. The "1" or "0" logic levels in the storage register are inputs to individual LM124 operational amplifiers. The operational amplifiers generate a continuous voltage output, +14 volts if receiving a "1" logic level from its storage register flip-flop or 0 volts, approximately, if receiving a "0" logic level. The LM 124 outputs go to the individual inputs of the CST and operate its circuitry.

The shift register flip-flops are not dedicated solely to an individual line or output. Logic levels are cycled through each flip-flop to the next one. The output line of each shift register flip-flop, going to an individual storage register flip-flop is the start of a group of components dedicated to a single command line or function. If a shift register flip-flop is defective, it results in improper commands, wrong commands, etc., and several circuits and systems are affected. Since this is not occurring, it can be concluded that the shift register is functioning properly and that the serial chain to examine for a malfunction begins with the input lines to the storage register flip-flop.

3.3 DEDICATED CIRCUITRY FOR CONE ANGLE SWITCHING

The circuitry dedicated solely to cone angle switching consists of HYBIC U32 storage register flip-flop Q_A, Q_B, and Q_C, and the three U11 operational amplifiers they are connected with respectively, and the three transistor switches in the CST. Hence, to each of the three cone angle command lines is dedicated the circuitry shown in Table 3 on page 3-5.

Re-examining the Cone Angle History, Table 1, it is seen that since encounter the CST has been commanded to cone angles C1 through C4 at various times. Turning to the Cone Angle Generation Logic, Table 2, it is seen that the circuitry dedicated to "Cone Angle Command A", going to pin C, has always been in the logic level 1 condition for all four cone angles. Since there was no anomaly in cone angles C1 and C2 and since the circuitry dedicated to "Command A" has never had to change state, it is presumed to be functioning properly.

Turning to the Logic Table and examining the logic states of "Cone Angle Command C", going to pin E, it is seen that, when in cone angle C1, the "Command C" dedicated circuitry was in logic level "1", and in cone angle C2, this circuitry was in logic level "0". Since no anomaly was observed in either of these cone angles,

Table 3. Dedicated Circuitry Table

Device	Cone Angle C'md A	Cone Angle C'md B	Cone Angle C'md C
Storage Resistor U21	Q _A	Q _B	Q _C
Op. Amp. U11	Pin 7	Pin B	Pin 14
Zener Diode	CR1	CR2	CR3
Transistor Switch	Q1	Q2	Q3

it can be presumed that the "Command C" dedicated circuitry is operating properly, both in the logic "1" and logic level "0" states.

Again, turning to the Logic Table and examining the logic states of "Cone Angle Command B", going to pin D, the following is seen:

- (1) In cone angles C1 and C2, "Command B" dedicated circuitry is in logic state "1". No anomaly occurs.
- (2) In cone angles C3 and C4, "Command B" dedicated circuitry is in logic state "0". An anomaly occurs in both cone angle positions.
- (3) "Command A" dedicated devices have not changed state from cone angles C1 through C4, and are assumed to be operating properly.
- (4) "Command C" dedicated devices were in the logic "1" state in cone angle C1, and in the logic "0" state in cone angle C2, where there was no anomaly. This circuitry is presumed, therefore, to be operating properly when in the logic "1" or logic "0" states when in cone angles C3 and C4 respectively, where the anomaly occurs.
- (5) The only circuitry uniquely related to the anomaly of cone angles C3 and C4 is the logic "0" state of the dedicated circuitry of "Command B". Therefore, a failure analysis of this particular dedicated circuitry should show the cause of the anomaly.

3.4 LOGIC STATE "0" FAILURE MODES OF "COMMAND B" DEDICATED CIRCUITRY

3.4.1 "Command B" Storage Register

The storage registers are 54L95 devices. These devices are inherently very radiation hard. If severe radiation damage occurred, the devices might stop changing logic state when commanded. This is not occurring, as evidenced by the "Command B" dedicated circuitry operating properly in cone angles C1 and C2. If the storage register Q_B flip-flop "leaked", placing a voltage at the input of its

connected LM 124 operational amplifier, the "Command B" line would always be in a logic "1" state. Since this is not occurring, it is safe to assume that the storage register is operating properly.

3.4.2 "Command B" LM124 Operational Amplifier

For a "Command B" logic "0" state failure, the "pin 8" operational amplifier of U11 would have to fail by having an offset voltage output which could cause the Q2 transistor in the CST "Command B" line to be at a state neither logic level "1" nor logic level "0". To do this, the operational amplifier offset voltage output (due to radiation damage) would have to be well over 3 volts to cause the Zener diode, CR2, in the CST, to conduct. LM 124 devices have been radiation tested at 125 Kilo Rad levels and offset voltage outputs, after radiation, of 4 to 10 millivolts have been observed. It is improbable that this device would still function properly, as it does when turned on in the C1 and C2 cone angles, if it had 3 volts or more of an offset voltage output due to radiation damage. Also, such an offset has never been measured in radiation testing. Therefore, it is safe to assume that the operational amplifier is operating properly.

3.4.3 "Command B" LM 103-3.0 Zener Diode

The LM103-3.0 Zener diode devices are very radiation hard, very stable, and tend to have very little, if any, leakage. To cause a logic "0" level failure, the diode would have to leak. If this situation occurred, and there was sufficient voltage reaching the base of Q2, Q2 could turn on just enough to allow some collector-emitter current to flow to pull down the collector to some indeterminate voltage, upsetting the ladder resistor network so that an improper cone angle is generated. In fact, this is exactly what is observed. When the C3 cone angle command, consisting of logic levels, 1, 0, 1 respectively is conducted to the Q1, Q2, and Q3 switches, the cone angle actually obtained is approximately C2. When the C4 cone angle is commanded, putting Q1, Q2, and Q3 in the logic states of 1, 0, 0 respectively, a cone angle between C2 and C3 is generated (see Cone Angle History, Table 1).

To check the validity of this failure mode hypothesis, a spare CST Serial No. 203, was set up in the Celestial Sensors laboratory. A conductor was wired across the CR2 Zener diode. The "Command B" input line to the CST was removed from the HYBIC output and a variable voltage was put on the "Command B" input line to the CST. The CST was turned on with a cone angle C3 command. Since cone angle C3 is achieved with Q1, Q2, and Q3 in the 1, 0, and 1 logic levels respectively, the CST was in cone angle C3 as long as the variable voltage on the "Command B" line was at zero.

To duplicate the anomaly being observed in Spacecraft 31, CST 205, which is a CST actual cone angle of C2 when the commanded cone angle is C3, using the shorted Zener diode and LM124 offset voltage output hypothesis, the variable voltage on the "Command B" line was raised slowly, and the change in cone angle was noted. The results are tabulated in Table 4, on the following page.

Table 4. Cone Angle Versus "Command B" Line Input Voltage
(Zener Diode Shorted; Cone Angle 3 Command On
Pins C, D, E)

Input Voltage	Cone Angle Position (volts)	Cone Angle
0	-0.013	C3
+0.1	-0.013	C3
+0.2	-0.013	C3
+0.3	-0.013	C3
+0.4	-0.013	C3
+0.5	-0.013	C3
+0.6	-0.013	C3
+0.7	-0.029	
+0.75	-0.082	
+0.78	-0.062	
+0.80	-0.212	
+0.82	-0.347	
+0.83	-0.422	
+0.84	-0.509	
+0.85	-0.638	
+0.857	-0.706	
+0.86	-0.754	

↑
 Anomaly
 Starts
 Occurring
 ↓
 C2

As can be seen by the above Table, even with a complete short of the CR2 Zener diode, greatly more offset voltage than is expected or has been experienced in radiation tests of the LM124 operational amplifiers must be produced to simulate the situation occurring in CST 205. Therefore, it is concluded that a Zener diode short or high leakage is not causing the anomaly.

3.4.4 "Command B" 2N2222A Transistor Switch

A failure mode involving this switch (Q2) exists when it leaks so it cannot be turned off completely. If, during Jupiter encounter, Q2 suffered severe bulk damage due to the Jupiter radiation field, high leakage between the collector and emitter would result. As long as the transistor was operated in the saturated mode (logic "1" level), proper operation of the cone angle generation circuitry would occur and no anomaly would be observed. But when Q2 must be turned off to go into cone angle C3 or C4, the leakage due to radiation damage would modify the resistor ladder voltage and, hence the resultant cone angle.

The above failure mode agrees with all of the observations of CST 205 performance observed through day 80-233. No anomalies occurred until after Jupiter encounter. Then, the anomalies occurred whenever Q2 was in the "off" or logic "0" state, where leakage could cause the anomalies observed in commanded cone angles C3 and C4. In cone angles C1 and C2, Q2 was in saturation and, indeed, no anomalies occurred. To test this hypothesis, a variable resistor was connected between the collector and emitter of Q2. With a cone angle C3 command status on Q1, Q2, and Q3, (1, 0, 1) the variable resistor was adjusted until

the CST was actually in cone angle 2. The Q2 collector voltage was measured and was 2.93 volts. The variable resistor was measured and was 6.96k Ω . Dividing the voltage by the resistance resulted in a leakage current of 421 μ amps.

The above test showed that if Q2 sustained radiation damage and developed leakage in the order of 400 μ amps, and could still be turned on into saturation, the anomalies observed could be exactly duplicated with a properly sized resistor across the collector and emitter of Q2.

To assess whether or not 2N2222A transistors developed leakage currents in the order of 200 to 400 μ amps due to radiation damage, Dr. Michael K. Gauthier, Sec. 365, Electronic Parts Engineering, was consulted. Dr. Gauthier has extensive files of radiation test results on 2N2222A transistor switches. He stated that if the 2N2222A's were made by Texas Instruments, it would be very improbable to have leakage currents more than 200 to 300 pico amps. However, if the 2N2222A's were made by Motorola, testing had shown some Motorola devices to have 200 μ amps or more leakage when radiated.

An investigation of the manufacturing records of CST 205 showed that it had originally been manufactured for the Viking Program as CST 104. This is shown by Figure 7, Hardware Review/Certification Requirement Form. The CST was retrofitted for the Voyager program and became CST 205. A check of the "As Built" records showed that the 2N2222A transistors came from Motorola and were purchased per JPL Specification PT 40068, attached. According to the Specification, the 2N2222A's were purchased as JAN-TX devices and do not appear to be specifically radiation hard.

Since a simulated 2N2222A leakage duplicated the anomalies observed in the Spacecraft, at least up to day 230, and since the leakage currents involved are within the range of leakage measured in radiation tests of these devices, it was concluded that the most probable cause of the CST 205 anomalies is radiation damage, incurred during Jupiter encounter, on the 2N2222A transistor in the Q2 position in the cone angle generating circuitry. Based on this conclusion, an alternate mode of operation (workaround) was investigated.

3.5 WORKAROUND

The spare CST was set up in the Celestial Sensor Laboratory. A 6.96k Ω resistor was wired across the collector-emitter of transistor switch Q2. The CST was commanded through all eight possible cone angle command states to observe where the actual cone angle would fall. The results are shown in Table 5, page 3-12.

A plot of the results of this table is shown in Figure 8, Cone Angle Achieved with Leakage Model Star Scanner.

From the Table it is seen that, if the simulation of the CST 205 condition is correct, cone angle C3 can be achieved. By commanding cone angle C4, the cone angle generating circuitry will actually produce cone angle C3.

PROJECT: MJS '77		SUBSYSTEM: Attitude Control		TYPE OF UNIT <input checked="" type="checkbox"/> FLT <input type="checkbox"/> NON-FLT <input type="checkbox"/> TEST <input type="checkbox"/> OTHER		COGNIZANT ENGINEER M. M. Birnbaum		EXTENSION 6555	SECTION 343	DATE 08/03/76	
REF. DES.:	PART NO.:	DWG. REV. LETTER	SERIAL NUMBER:	NOMENCLATURE			FINAL INSPECTION REPORT NO.	OPERATING TIME OR CYCLES	WEIGHT (GRAMS/KILOGRAMS)		
2007 CT1/2	10062349-2	F*	205	Canopus Star Tracker and S.E. Hood No. 201 (Goes with Baffle No. 205) Image dissector tube changed out after receipt from VO-75 project. 342 hours of operating time were recorded on Canopus Star Tracker (S/N 104) before it was sent to Honeywell, Inc. for retrofitting as S/N 205. S/N 205 is functionally and mechanically interchangeable with other units.			A 15533	261.4 hours	0.230 lbs		
CHECK APPLICABLE ANSWER AND GIVE NECESSARY EXPLANATION IN REMARKS COLUMN			YES	NO	N/A	REMARKS AND/OR LISTED INFORMATION					
1.	Are all drawings and specifications complete, approved, released and frozen?		<input checked="" type="checkbox"/>	<input type="checkbox"/>	<input type="checkbox"/>	12. List the ECR's against this hardware that have not been closed. <input checked="" type="checkbox"/> NONE					
2.	Do the released drawings and specifications reflect all approved changes? *		<input type="checkbox"/>	<input checked="" type="checkbox"/>	<input type="checkbox"/>	13. List Waivers that apply to this hardware. <input type="checkbox"/> NONE 40007, 40445, 40449, 40527, 40345, *2. "As Built" list is correct. Parts list of Dwg. #10062349 must be changed per ECI No. 87484					
3.	Is this hardware identical to the other hardware delivered to SAF? (If no, state in Remarks where differences are documented.) *		<input type="checkbox"/>	<input checked="" type="checkbox"/>	<input type="checkbox"/>	14. List MRB Nos. that required Section Manager decision <input checked="" type="checkbox"/> NONE *3 S/N 205 is a retrofitted V075 Tracker. Difference between it and remainder of Trackers is in the mechanical and fabricating details and is minor. Documented in -2 configurations of 10062349.					
4.	Does the hardware meet the requirement of the Interface Control Drawings?		<input checked="" type="checkbox"/>	<input type="checkbox"/>	<input type="checkbox"/>	15. List the open PFR's affecting this hardware. <input checked="" type="checkbox"/> NONE					
5.	Have all discrepancies and MRB's been dispositioned and agreed to by Engr/QA?		<input checked="" type="checkbox"/>	<input type="checkbox"/>	<input type="checkbox"/>	16. List open PFR's on other hardware of this type that may affect this hardware. <input checked="" type="checkbox"/> NONE					
6.	Has complete as-built list information been submitted to Section 356?		<input checked="" type="checkbox"/>	<input type="checkbox"/>	<input type="checkbox"/>	17. List Test Result Summary Forms submitted to Section 294. <input type="checkbox"/> NONE TRSF's Nos. J-063, J-104, J-210					
7.	Are all radiation requirements satisfied and all required radiation modifications incorporated?		<input checked="" type="checkbox"/>	<input type="checkbox"/>	<input type="checkbox"/>	18. Complete MJS77 subsystem power data sheet. See attached sheet					
8.	Have all required TA Tests and analysis been completed?		<input checked="" type="checkbox"/>	<input type="checkbox"/>	<input type="checkbox"/>						
9.	Is all subsystem level testing complete?		<input checked="" type="checkbox"/>	<input type="checkbox"/>	<input type="checkbox"/>						
10.	Has applicable telemetry calibration data been submitted to Section 293?		<input checked="" type="checkbox"/>	<input type="checkbox"/>	<input type="checkbox"/>						
11.	Is this hardware fully acceptable for flight?		<input checked="" type="checkbox"/>	<input type="checkbox"/>	<input type="checkbox"/>						
COG. ENGR. <i>M. M. Birnbaum</i> DATE 08/03/76			DIV. REP. <i>J. J. Davis</i> DATE 8-3-76			ATTACH ADDITIONAL SHEET IF NECESSARY					
COG. ENGR. SUPT. <i>M. M. Birnbaum</i> DATE 8-3-76			DIV. QA ENGR. <i>J. J. Davis</i> DATE 8-3-76			S/C SYS. MANAGER		DATE		SAF QA ENGR	DATE
FIGURE 7. HARDWARE						REVIEW/CERTIFICATION		REQUIREMENT FORM			

3-9

Figure 7. Hardware Review/Certification Requirement Form

b. Paragraph 3.3, change notification of JPL to notification of HRC.

c. Paragraph 3.5.2, change from five (5) copies to two (2) copies.

2.3 ZPP-2073-8037-C - Test Specifications, Transistors, Silicon, NPN, 2N2219A and 2N2222A

Exceptions:

None.

Handwritten notes:
None - 1/11/68
[unclear] [unclear] [unclear]

JET PROPULSION LABORATORY CALIFORNIA INSTITUTE OF TECHNOLOGY

TRANSISTOR, HIGH SPEED SWITCH, NPN, SILICON (2N2222A)

PT40068

SHEET 2 OF 2

Table 5. Cone Angle Achieved with Leaky Q2

Commanded Cone Angle	Cone Angle Position Readout <u>With Leakage</u> (volts)	Cone Angle Position Readout <u>No Leakage</u> (volts)
C1	-1.47	-1.46
C2	-0.78	-0.75
C3	-0.70	0
C4	0	+0.75
C5	+1.46	+1.46
C6	+1.68	+1.68
C7	+1.68	+1.68
C8	+1.68	+1.68

In the above model and analysis, there is one inconsistency. Looking at the Cone Angle History, Table 1, it is seen that on day 80-121 (30 April 1980), the CST was commanded to cone angle C4. It went actually to about 25 percent beyond C2 (between C2 and C3), as evidenced by the DN95. The leakage model used to simulate the present status of CST 205, has the actual cone angle going to C3, a DN of 128, when C4 is commanded. Why the discrepancy?

Several possible reasons for the difference between the leakage model in the Laboratory and the CST 205 situation of 30 April 1980 are:

- (1) Annealing has taken place so the leakage is less now than formerly.
- (2) The model is only approximate and does not contain components for other radiation damage effects which might have occurred.

3.6 RECOMMENDATION

There is enough of a discrepancy between the 2N2222A failure model and the observed results to be concerned. Since there are only two measured anomalous data points, cone angle C4 in April 1980, and cone angle C3 in July 1980, and the failure model only duplicates one of them, C3, a recommendation was made that the Voyager Spacecraft be commanded to go through all eight possible cone angles so that a complete set of cone angles could be obtained on which a more consistent model could be built. Measuring all of the cone angles, especially cone angle C5, would either prove or disprove the 2N2222A failure mode theory. In cone angle C5, the logic states of Q1, Q2, and Q3 (see Table 2) are 0, 1, 1, respectively. Q2 is in the "one" state and is saturated. Therefore, if it is causing the trouble, in this state the anomaly should disappear and a proper cone angle C5 should be achieved.

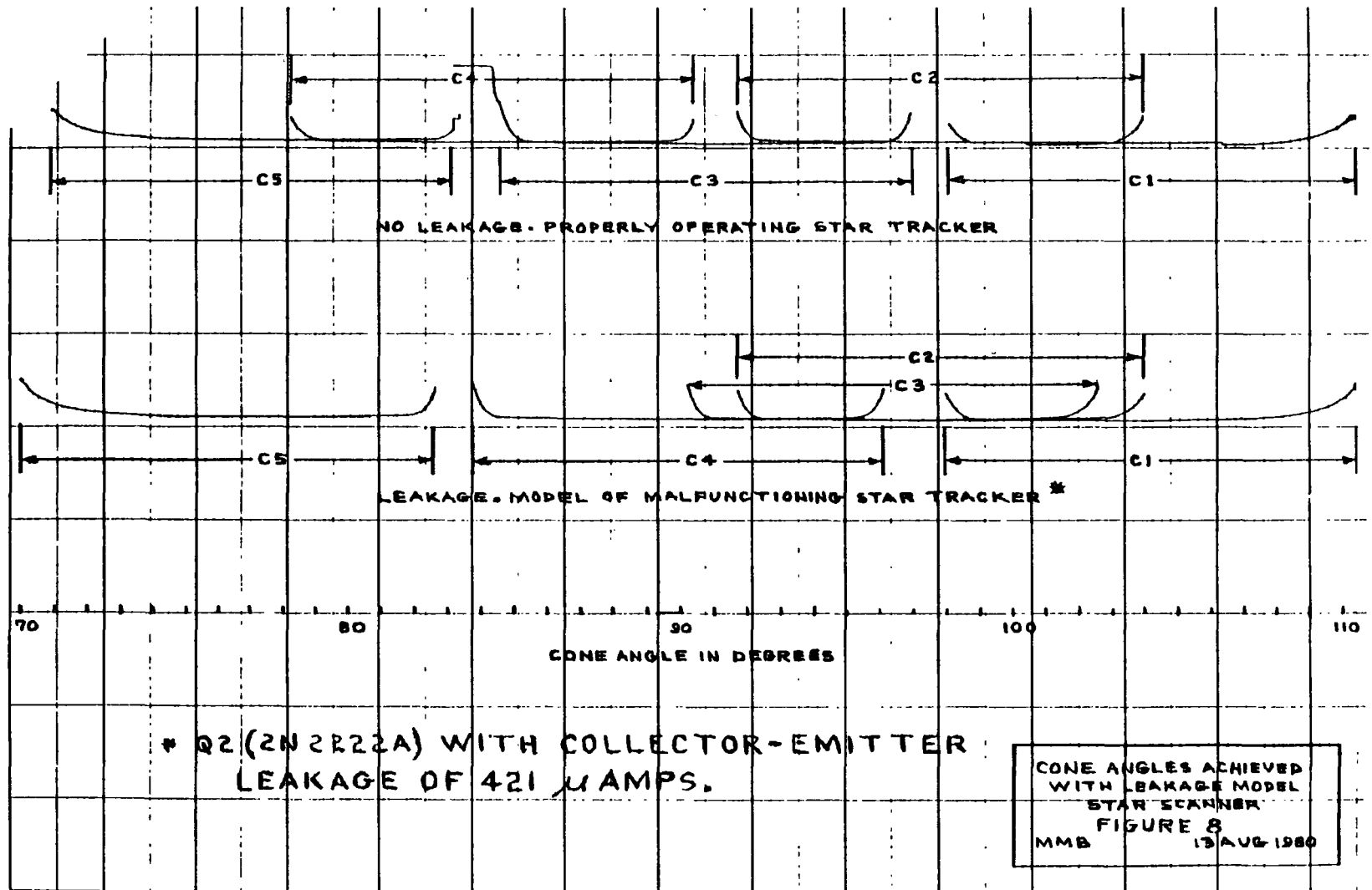


Figure 8. Cone Angles Achieved with Leakage Model Star Scanner

3.7 CST S/N 205 CONE ANGLE MEASUREMENTS

On day 80-233, Voyager Spacecraft 31 CST S/N 205 was commanded through all eight possible cone angles. The received telemetry data is shown in Table 6, below.

3.8 CONE ANGLE MEASUREMENT CONCLUSIONS

From Table 6, it is seen that the CST did not attain a proper cone angle C5. This means that the 2N2222A postulated as being unable to be turned off (Q2) is not the cause of the problem. In cone angle C5, Q2 is in the saturated mode and cannot cause the observed anomaly.

With all of the cone angles actually measured, it is seen that only the top half of the cone angles (C1, C2, partial C3) can be achieved. This indicates a fault in either the LM 108AH reference amplifier (U1 in Figure 5) or in the SDT 5553 high voltage cone angle deflection transistor (Q5 in Figure 5), or in the UZ 8770 Zener diode (CR5 in Figure 5). These three devices were analyzed in detail.

Table 6. Voyager Spacecraft 31-CST Cone Angle-Intensity History on Day 80-233 (20 August 1980)

Cone Angle Commanded	Cone Angle Measured DN	Correct Cone Angle DN	Intensity (Canopus) DN
C1	45.40	44-46	
C2	80.45	84-86	
C3	88.17	127-129	
C4	92.00	165-167	
C5	96.48	206-208	
C6	101.4	--	
C7	106.5	-	
C8	111.02	-	
C3 ← (80-234) ↷	87.48	127-129	186.10

SECTION 4

CONE ANGLE DEFLECTION SYSTEM INVESTIGATION

4.1 LM108AH REFERENCE AMPLIFIER U1

A failure of U1 could account for the observed cone angle anomaly only if the reference amplifier were capable of outputting negative voltages but not positive voltages. A schematic of the LM108AH, shown in Figure 9, LM108AH Schematic was obtained and reviewed. Further inspection showed an output PNP transistor (Q19) which, if leaky, could possibly prevent positive voltage outputs. Consultation with H. Stuart Dodge (Sec. 365 Parts Specialist) disclosed that this failure mode had never occurred during any of the LM108AH radiation tests and was not considered likely. Further tests in the Laboratory, on the spare CST, by simulating the observed failure by limiting the positive output excursion of the U1 reference amplifier, were not successful in duplicating the observed anomalous cone angle DN readings observed in Table 6.

4.2 CONE DEFLECTION TRANSISTOR, SDT 5553 (Q5)

The high voltage transistor, Q5, shown in Figure 5, is a SDT 5553 device which is not radiation hard and is known to exhibit radiation sensitivity because of its high voltage construction (i.e., wide base region). These devices are also known to exhibit wide performance variations from lot to lot. Both cone angle deflection transistors, Q5 and Q7, are housed in a tungsten box within the CST to reduce the radiation levels to which they will be exposed.

A failure mode which can cause the anomalous results seen is a collector-to-emitter leakage in transistor Q5. With this failure mode, cone angles C1 and C2 are not affected since they require Q5 to be driven towards saturation. However, cone angles C3 through C5 will not be correct since they require Q5 to be driven towards cutoff. The range of the collector current in Q5 is from 191 μ amps to 1050 μ amps.

4.3 SIMULATION OF SDT 5553 (Q5) FAILURE MODE

A simulation of excess leakage in Q5 was performed using the spare CST. A variable resistor was placed across the collector and emitter leads of the transistor. When the resistor was 40K Ω , resulting in 948 μ Amps collector-emitter leakage current, the C1 to C8 cone angles, achieved in response to cone angle commands, were almost identical to those actually observed in the Voyager Spacecraft 31 anomalous CST. A plot of the DN's from the anomalous CST and from the Laboratory CST is shown in Figure 10, Cone Angles Commanded Versus DN Achieved For Q5 Collector-Emitter Leakage.

If there was a Q5 base-to-ground leakage or base-to-emitter leakage, instead of the assumed collector-to-emitter leakage, the resultant change of base dc voltage level could cause the transistor to be partially turned on all of the time. This failure mode was investigated by putting a resistor from Q5 base to ground. When the base-to-ground resistor was 667K Ω , resulting in 110 μ amps

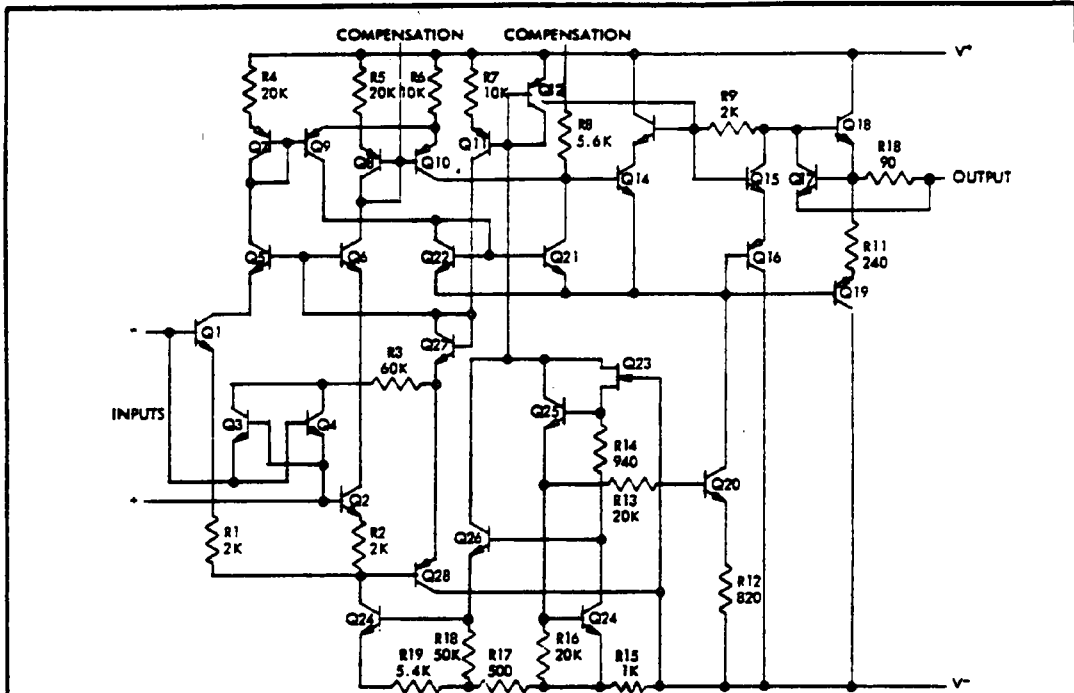
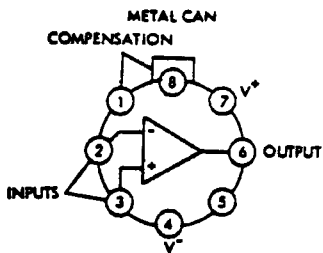
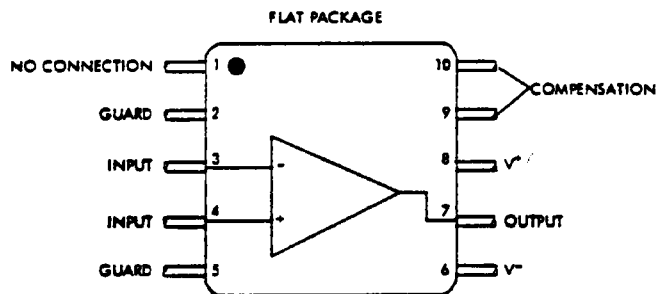


Figure 30. Schematic Diagram (LM108, LM108A)(NSC)



NOTE: Pin 4 connected to case.
TOP VIEW

Figure 31. Connection Diagram (LM108H, LM108AH)



NOTE: Pin 6 connected to bottom of package
TOP VIEW

Figure 32. Connection Diagram (LM108F, LM108AF)

LM 108 AH SCHEMATIC FIGURE 9

JET PROPULSION LABORATORY		CALIFORNIA INSTITUTE OF TECHNOLOGY	
	REV	TITLE	ST 11499 REV E
SHEET		MICROCIRCUIT, LINEAR	SHEET 19

UNCLASSIFIED

Figure 9. LM108AH Schematic

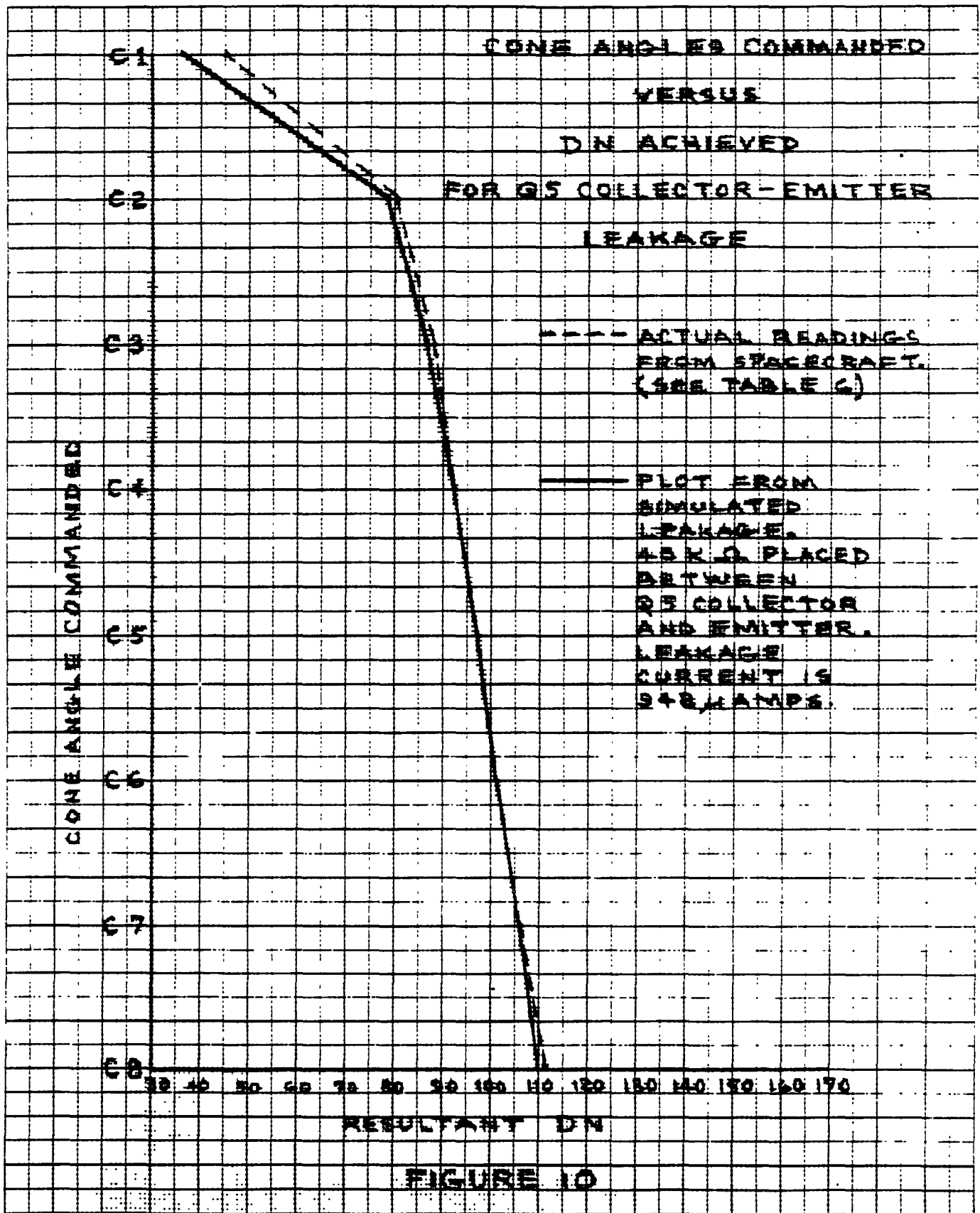


Figure 10. Cone Angles Comanded Versus DN Achieved for Q5 Collector-Emitter Leakage

leakage current, the resultant plot of "Cone Angles Commanded Versus DN Achieved" was identical with the case above, where a 40K Ω resistor was placed between the collector and emitter of Q5. Approximately the same results would be obtained if a leakage resistor was placed between the Q5 base and emitter.

4.4 ZENER DIODE, UZ8770 (CR5)

The same cone angles commanded versus DN's achieved, that are presently existing in the Voyager Spacecraft CST, can be obtained by assuming a leakage path across the CR5 Zener diode connected to the base of Q5 through a 10K Ω resistor. (See Figure 5.) If a 510K Ω resistor is placed across the CR5 Zener diode, the identical DN's for commanded cone angles is achieved as when a 40K Ω leakage resistor was placed across the Q5 collector-emitter leads.

In assessing which component, the CR5 Zener diode or the Q5 SDT 5553 transistor is causing the anomaly, the diode was ruled out. The diode is a UZ 8770 and is very radiation hard. No leakage failures similar to the failure mode postulated have been experienced - either by radiation testing or otherwise. Under severe radiation of up to 250 kiloRads, the Zener voltage changes by 20 millivolts. It is considered highly unlikely that the Zener diode would fail by leakage. If it received a large voltage spike, it would short out completely and cause different cone angles than the ones being observed from the Voyager Spacecraft.

The SDT 5553, Q5 position, transistor is left as the cause of the cone angle anomaly. In some manner, a collector-emitter or a base-emitter or base ground leakage has developed. Probably only Q5 has suffered damage. Q7 appears to be operating properly because of the ability to command cone angles 1 and 2 correctly. Q7 provides opposite polarity voltage to one of the cone deflection plates in the image dissector tube. Since the drive signal for Q7 comes from the collector of Q5, anomalous operation of Q5 in cone angles C3 through C5 will result in improper deflection voltages from Q7 also, even though Q7 is undamaged.

4.5 SDT 5553 TRANSISTOR DESIGN AND USE IN CST

The radiation sensitivity of the SDT 5553 transistor became well known during the parts screening that was done on the Voyager program. The SDT 5553 transistor was one of the least radiation hard electronic components used on the Voyager Spacecraft. Due to the fact that the SDT 5553 is a high voltage transistor, used to generate up to plus and minus 60 volts to the image dissector tube cone angle deflection plates, no radiation hard replacement was available.

Extensive radiation testing of these transistors was done. It was found that if radiated to a small dose of five to ten kiloRads the SDT 5553 transistors which were extremely susceptible to radiation suffered drastic drops in their h_{FE} while the sturdier ones showed little change at these radiation levels. It was also found that most of the radiation damage could be eradicated by annealing the radiated transistors at a temperature of 150 degrees C for 96 hours.

Radiation analyses of the CST showed that the SDT 5553 transistors would receive a dose of 75 kiloRads, if the Jupiter radiation was as expected. Project guidelines were that the expected radiation be doubled, and all electronic components be designed, shielded, or tested to operate at twice the expected radiation dose. In this case, the SDT 5553 transistors, by their inherent design and characteristics, could not operate, after 150 KiloRads radiation dose, without unacceptable degradation. It was decided, therefore, to design a tungsten box in which the transistors would be placed, to reduce the radiation they would receive to an acceptable level. A shielding analysis was done and a tungsten box, 0.150 inch thick on each side was designed to hold the SDT 5553 transistors. The box reduced the radiation dose the transistors would receive to 2.5 kiloRads expected; 5.0 kiloRads at twice the expected radiation. The design of the tungsten box is shown in Figure 11, Tungsten Box For SDT 5553 Transistors.

To insure the survivability of the SDT 5553 transistors, a radiate and anneal test/screening program was initiated. All SDT 5553 transistors were screened and tested to determine their parameters, especially h_{FE} . They were then radiated to a dose of 5 kiloRads and their parameters measured again. Those showing no or minimal change were annealed and their parameters were measured again. The ones with the smallest parameter changes were used in the CST and installed in the tungsten shielded boxes.

4.6 CAUSES OF SDT 5553 FAILURE

After it was determined that the cause of the CST cone angle problem was an SDT 5553, in position Q5, the parts specialists at JPL were consulted who had done the work on its screening, radiating, and annealing. They stated that in all of their testing experience with the SDT 5553, they had never seen a failure due to radiation as was being described, namely a large base-emitter leak of over 100 μ amps, or a collector-emitter leak of over 900 μ amps. In the test program, SDT 5553 transistors had been radiated to 250 kiloRads and collector-emitter leakages of up to 12 μ amps had been noted on some units. Also, it was pointed out by the radiation testing group that the transistors were heavily shielded and were subjected to less than 5 kiloRads during Jupiter flyby. This dose level was too low to do any damage, in view of the radiate and anneal selection process that was used. It was suggested that the packaging of the transistors in the tungsten box be investigated, especially the sleeving around the transistor leads that exited through holes in the base of the box.* This suggestion was taken, and the sleeving material used around the SDT 5553 leads, Delrin AF, was investigated in great detail as a possible mechanism by which a base-emitter or collector emitter leakage could occur.

* This suggestion was made by W. E. Price of the Electronic Parts Engineering Section, who was responsible for the radiation testing program on Voyager. His experience indicated that many plastics decomposed when radiated.

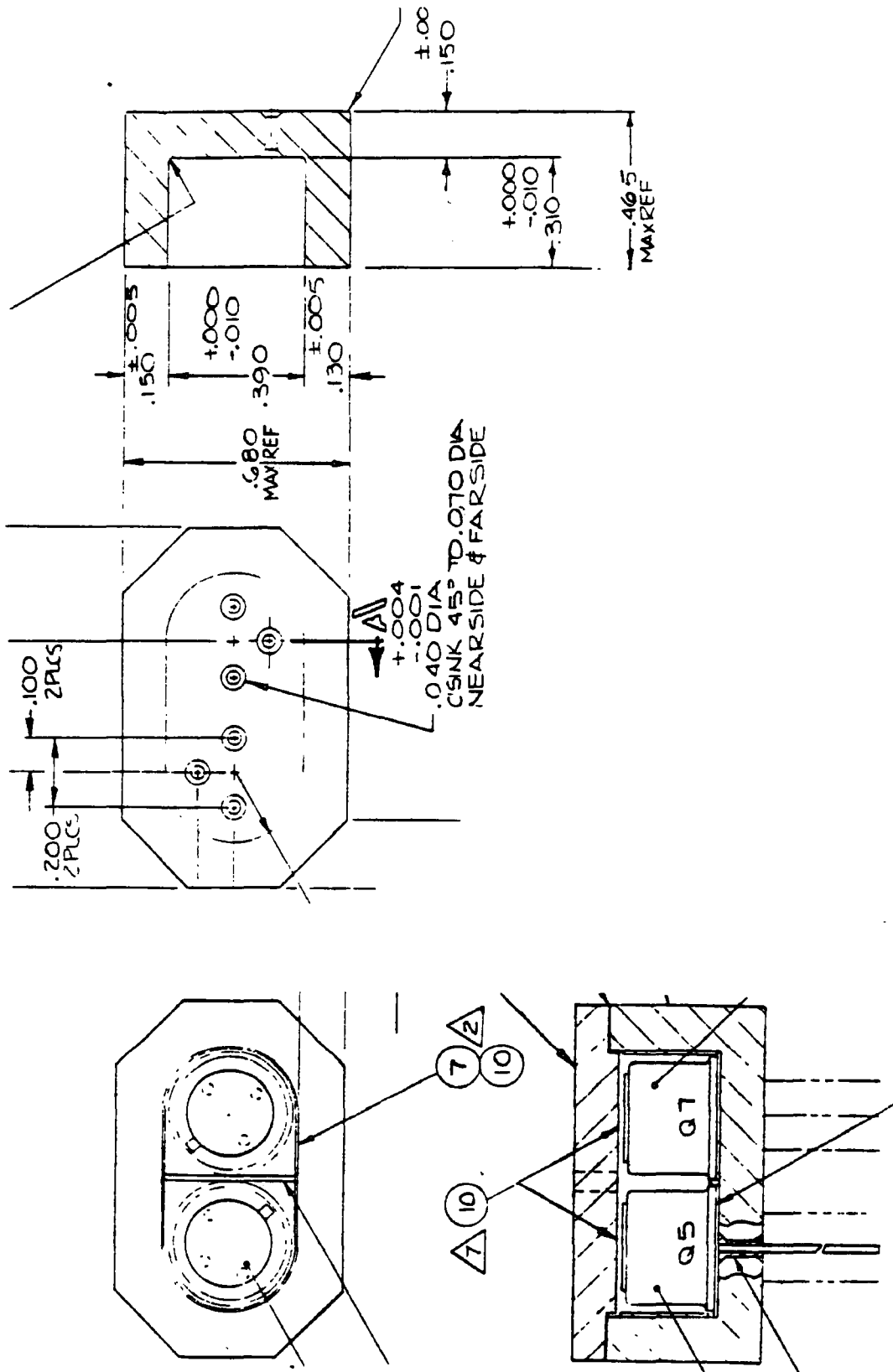


Figure 11. Tungsten Box for SPT 5553 Transistors

SECTION 5

DELTRIN AF INVESTIGATION

5.1 DELTRIN AF SLEEVE DESIGN

Delrin AF sleeves, machined from a block of Delrin AF, are used to insulate the SDT 5553 transistor leads as they exit through the wall of the tungsten box. The tungsten wall is 0.150 inch thick. The holes in the tungsten box are 0.040 inch in diameter, countersunk at both ends. The sleeves are machined to fit the countersunk volume at the inner surface of the box, so that, inside the box, the sleeving surface is flush with the inner surface of the tungsten box. The sleeve length is 0.150 inch. Its outside end, exposed to the high radiation is flush with the outside surface of the tungsten box. The countersunk volume of the box is filled with an alumina-loaded polyurethane after the tungsten box, SDT 5553 transistors, and Delrin AF sleeving are assembled. The design of the Delrin AF sleeve is shown in Figure 12, Delrin AF Sleeve Design.

The tungsten box design and hole pattern layout produce, for each sleeve, a longitudinal tungsten-Delrin AF interface about 0.150 inch long. The collector and base sleeves for the same transistor are separated by about 0.10 inch of solid tungsten in the middle of the box wall, and by about 0.11 inch path length along the outer tungsten surface.

5.2 DELTRIN AF DESCRIPTION*

Delrin AF is composed of oriented Teflon fluorocarbon fibers uniformly dispersed in Delrin 500 acetal resin. It is made by DuPont. Delrin 500 is designed for the injection molding process. It is used in mechanical parts, gears, bearings, housings, and personal items. Delrin AF is specifically formulated to have an extremely low friction surface. It is one of the most slippery solid materials and is widely used in moving parts where low friction and low wear are important considerations and where lubrication is impractical.

Telephone discussions with DuPont product specialists brought out the following facts:

- (1) In its manufacturing process, the Delrin AF can have microvoids which can be seen easily with a magnifying glass.
- (2) Delrin AF is particularly vulnerable to Ultra-violet light and to gamma rays. In the presence of either Ultra-violet light or gamma rays, Delrin AF depolymerizes, forming formaldehyde.

*The material for this section was gathered by John W. Winslow, JPL Parts Specialist, Section 352. He contacted DuPont and other specialists and described the failure mechanisms of Delrin.

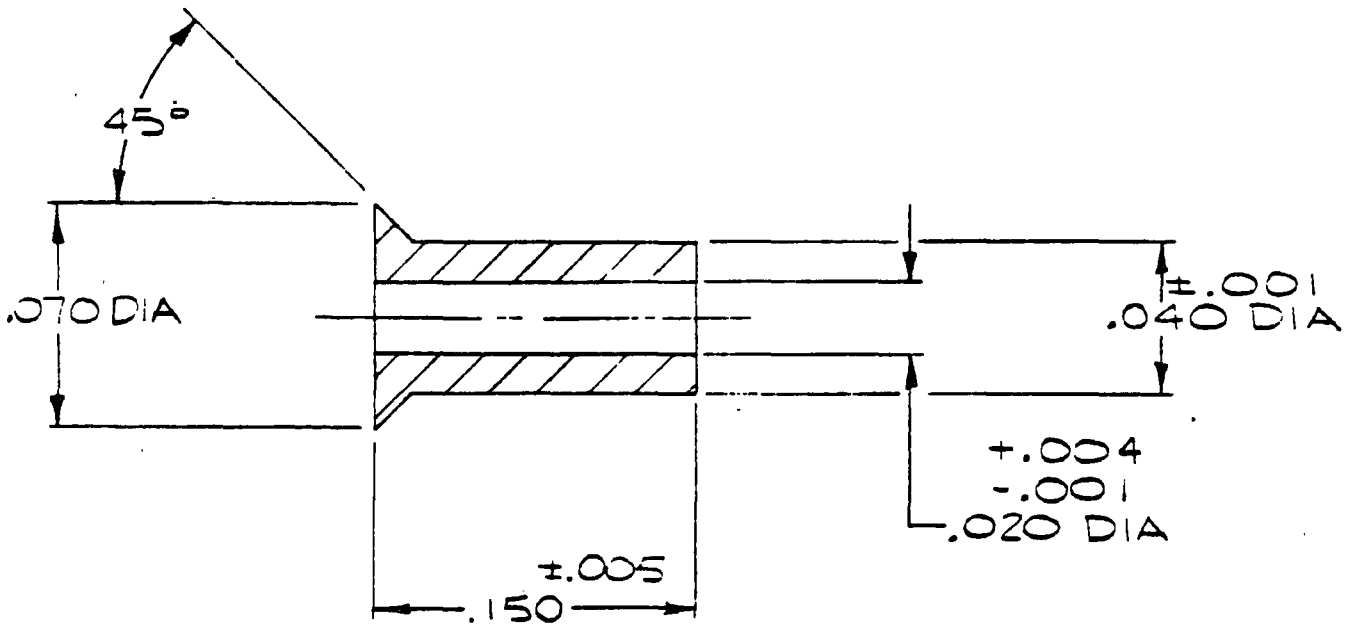


Figure 12. Delrin AF Sleeve Design

Exposure of Delrin AF to ionizing radiation would be expected to generate considerable quantities of formaldehyde. The Jupiter radiation field consists of particles much more energetic than Ultra-violet photons, and would have more than enough energy to break the backbone bond (The C-O bond) of the Delrin 500 resin. As the Delrin 500 molecules depolymerized, formaldehyde would be produced.

Radiation products of the Teflon in the Delrin 500 are uncertain due to lack of knowledge as to the effects arising from the presence of oxygen atoms in the Delrin 500 backbone chain. It would be quite reasonable, however, to expect exposure to the radiation belts around Jupiter (and also around the Earth) to produce some H₂ from the Delrin 500, and some F₂ from the teflon, and especially along the interfaces between the Delrin 500 and the Teflon fibers, to produce a weak solution of HF (Hydrofluoric Acid) in formaldehyde. Such a solution would be somewhat conductive electrically, and could produce a high resistance conductive path between the transistor base, emitter, and collector leads as they exited the tungsten box. If the HF formed a path between the collector and emitter leads or between the base and emitter leads, acting in a random way, the observed failure mode could occur.

5.3 ELECTROSTATIC CHARGING OF DELRIN AF SLEEVES

One of the failure modes investigated was by the mechanism of electrostatic charge buildup on the tungsten box and discharge through the Delrin AF sleeve to the SDT 5553 transistor lead. The tungsten box was epoxyed to the printed circuit board on which it was mounted and the box was not grounded. This was done because charge buildup inside the CST was expected to be very small, and it was not desired to place a ground potential so close to the plus and minus 60 volt potentials on the collector and emitter leads of the transistor.

The electrostatic discharge analysis is shown in Appendix 1, Electrostatic Charging of the Voyager Star Tracker Delrin AF Sleeve for the Case of a Floating Tungsten Spot Shield. The Analysis shows that the current leaking across the base lead Delrin AF sleeve due to electrostatic charge buildup is always less than one nanoamp, thus it will not cause any damage. The calculated peak voltage in the tungsten box, however, is about 350 volts, producing about 48 volts per mil of electric field inside the Delrin AF. The Delrin AF has a dielectric strength of 1700 volts per mil, and the sleeve wall is 10 mils thick. It is possible that, due to the radiation damage at Jupiter causing HF to be formed and etch a path from the leads to the tungsten box (across the Delrin AF sleeve), and due to the possible microvoids when the DELrin AF was manufactured, and scratches and cracks when the sleeve was machined, that an electrostatic discharge occurred and burned a high resistance path across a sleeve to the tungsten box. This phenomena may not have occurred when the Spacecraft went through the van Allen belts, and the HF-Formaldehyde formed then, eventually evaporated. At Jupiter, the vastly larger radiation field could produce a much greater quantity of HF-Formaldehyde. The HF, coupled with flaws in the Delrin AF, and possible electrostatic discharge through the flawed sleeve area, could explain the SDT 5553 transistor leakage and the stability of the leakage path. (In the future, even inside equipment, all shielding boxes will be grounded.)

5.4 PROPOSED SCENARIO OF EVENTS CAUSING FAILURE

The sequence of events proposed to account for the observed CST behavior has the following postulates:

- (1) One or more of the Delrin AF sleeves around the base, collector, and emitter leads of the SDT 5553 transistor is assumed to have been flawed - through some combination of microvoids in the material and/or scratches or cracks when the sleeves were machined from Delrin AF.
- (2) Passage through the Earth's van Allen belts is assumed to have generated enough HF-formaldehyde solution to convert a path (in combination with some flaw or flaws) into an active but still very high resistance leakage path.*
- (3) This path is assumed to have returned to a highly insulated state during the Earth-Jupiter leg of the spacecraft flight. This could occur through simple evaporation of the conductive solution. Alternatively, acid attack on the tungsten and/or copper surfaces where the path emerged from the Delrin AF, might also have accomplished the same result. It should be noted that the return of only a small portion of the path to the insulating state would give the appearance of a cure - the malfunction would disappear.
- (4) Finally, passage through the Jovian radiation belt is assumed to have invoked some combination of the dielectric breakdown and acid-forming mechanisms which either reestablished the old conductive path, or else established a new one.

The above sequence of events has one shortcoming. It does not explain in any obvious way why the CST cone angle variations did not appear until twelve days after launch. It would seem that the malfunction should have appeared promptly upon passage through the van Allen belts.

The failure mode mechanism described above, though not perfect, accounts for most of the major features of the observed CST malfunctions, both early in the mission and when passing through the Jovian radiation field. The failure mode model envisions the generation of a leakage path across the Delrin AF sleeves insulating the base, collector, and emitter leads of the Q5 SDT 5553 transistor from its tungsten box, caused by passage of the Spacecraft through the Earth's van Allen radiation belts. The leakage path is then envisioned as having disappeared slowly, due either to evaporation of the radiation chemistry products, or else as a result of the acid attack on the tungsten and copper leads. The path is then envisioned as being regenerated, or replaced, due to the much larger radiation dose received as the Spacecraft passed through the Jovian radiation field.

* There was an unexplained cone angle anomaly which occurred twelve days after launch. The cone angle (C4) which had been stable, began to vary by one to two degrees. This condition existed for about twenty days until the CST was switched to cone angle C3.

If the mechanism invoked by the Jovian radiation field was the generation of the conductive solution of HF in formaldehyde, the expectation would be for the leakage path to disappear gradually. In this event, the rate of disappearance would be quite slow - at least as slow as the rate observed during the Earth-Jupiter part of the flight. The gradual disappearance would be expected to continue, at least until further high energy radiation exposure(s) occurred.

If, on the other hand, the mechanism invoked at Jupiter was catastrophic dielectric breakdown through the microvoids, scratches, or cracks in the Delrin AF when it was manufactured and then machined, no further change in the leakage resistance would be expected. A carbonized path would have been burned through the Delrin AF. The fact that the resistance has remained constant from its initial sensing in April 1980 to the present, argues in favor of this mechanism.

No change in leakage resistance is expected unless the CST is exposed to more radiation. When passing by Saturn, the CST will be exposed to a radiation field fluence only 1/30,000 that of Jupiter. It is not expected to cause any further change in the existing leakage resistances. Therefore, the CST should continue to operate with its cone angle circuit unchanged, as it has from Jupiter to Saturn.

SECTION 6

CST 205 INTENSITY VARIATION INVESTIGATION

6.1 INTENSITY HISTORY AFTER ANOMALY DISCOVERY

After the CST was commanded to go into all of its possible cone angles on days 80-233 and 80-234 (See section 3.7), it was decided to verify that the back-up CST was still useable. The spacecraft was commanded to switch to the back-up CST and this CST was operated for days 80-234 and 80-235. The back-up CST functioned properly and it was commanded through all of its cone angles. Cone angle DN's were recorded, and star intensity DN's were recorded in cone angle C3. When these back-up CST tests were completed, the spacecraft was commanded to switch back to the primary CST, S/N 205, with the cone angle defect. The cone angle-intensity history of both of these operations is shown in Table 7, below.

Table 7. Voyager Spacecraft 31-CST Cone Angle-Intensity History on Days 80-234 Through 80-242

Date	Cone Angle Commanded	Cone Angle Measured DN	Correct Cone Angle DN	Intensity (Canopus) DN
Back-up CST				
80-234 to 80-235	C3	127.9963	128	179.9291
80-235	C4	167.8571	172	--
80-235	C5	211.0000	216	--
80-235	C1	45.4898	40	--
80-235	C2	84.7692	84	--
80-235	C3	127.92	128	180.1622
Primary CST				
80-235	C3	85.6667	128	183.00*
80-235 to 80-242	C5	96.1339	216	186.9905
80-242 to Present	C8	109.7231	---	190.9889

*The CST was only on for eight minutes when this reading was taken. It was then switched to C5. After warm-up, a reading of 186 would be expected.

When the CST was switched to cone angle C8, it was noticed that the DN was almost 191 instead of the expected 186 to 187. Higher DN's mean lower signal (see Figure 4). Therefore, there was some concern that in addition to the cone angle problem, the CST image dissector tube had also lost sensitivity in the area of cone angle C2 to C3. To be able to set proper intensity thresholds, this effect had to be investigated. It was noted that as the cone angle was commanded from cone angle C3 to C5 to C8, that the intensity reading kept decreasing (DN's becoming larger). It was suspected that this was due to electro-optical defocusing inside the image dissector tube, due to the incorrect voltages on the cone angle deflection plates. To ascertain that this theory was correct, the laboratory CST was set up with a 667 kilo-ohm leakage resistor between the base lead and ground. With this configuration, the laboratory CST, S/N 203, duplicated every cone angle reading coming from the spacecraft CST, S/N 205, as the spacecraft CST was commanded through cone angles C1 through C8.

6.2 INTENSITY PROBLEM SIMULATION

An intensity test was done. The laboratory CST was placed on the Canopus simulator; the simulator was adjusted for 1 x Canopus. A series of intensity readings were taken as the CST was commanded from cone angle C3 through C8 (in these cone angles, the Canopus image was always in the field-of-view. The results of this intensity test are shown in Table 8, below.

Table 8. CST, S/N 203, Intensity Readings With Defective Cone Angle Circuit

Cone Angle	FDS Intensity (Volts)	DN*	ΔDN
C3	8.62	179.3	0
C4	8.64	179.8	0.5
C5	8.67	180.3	1.0
C6	8.70	181.0	1.7
C7	8.72	181.5	2.2
C8	8.75	182.1	2.8

Test Conditions:

1 x Canopus used at 92 degrees cone angle
 667 kilo-ohms between Q5 SDT 5553 base lead and ground

$$*DN = \frac{\text{Voltage} - 0.012}{0.048}$$

It is seen that, for CST 203, the intensity DN decreases by 2.8 in going from C3 to C8. In the spacecraft CST, a change from 186 (after warm-up) to 191 was recorded, as a Δ DN of 5. This does not occur in properly functioning CST's, as shown by the intensity readings of Table 1, cone angles C4, C3, C2, where readings were taken for 164 days after launch. Cone angle C1 has an intensity DN reading of 180.1, but this is between 164 to 181 days after launch, and the image dissector photocathode has degraded and lost sensitivity.

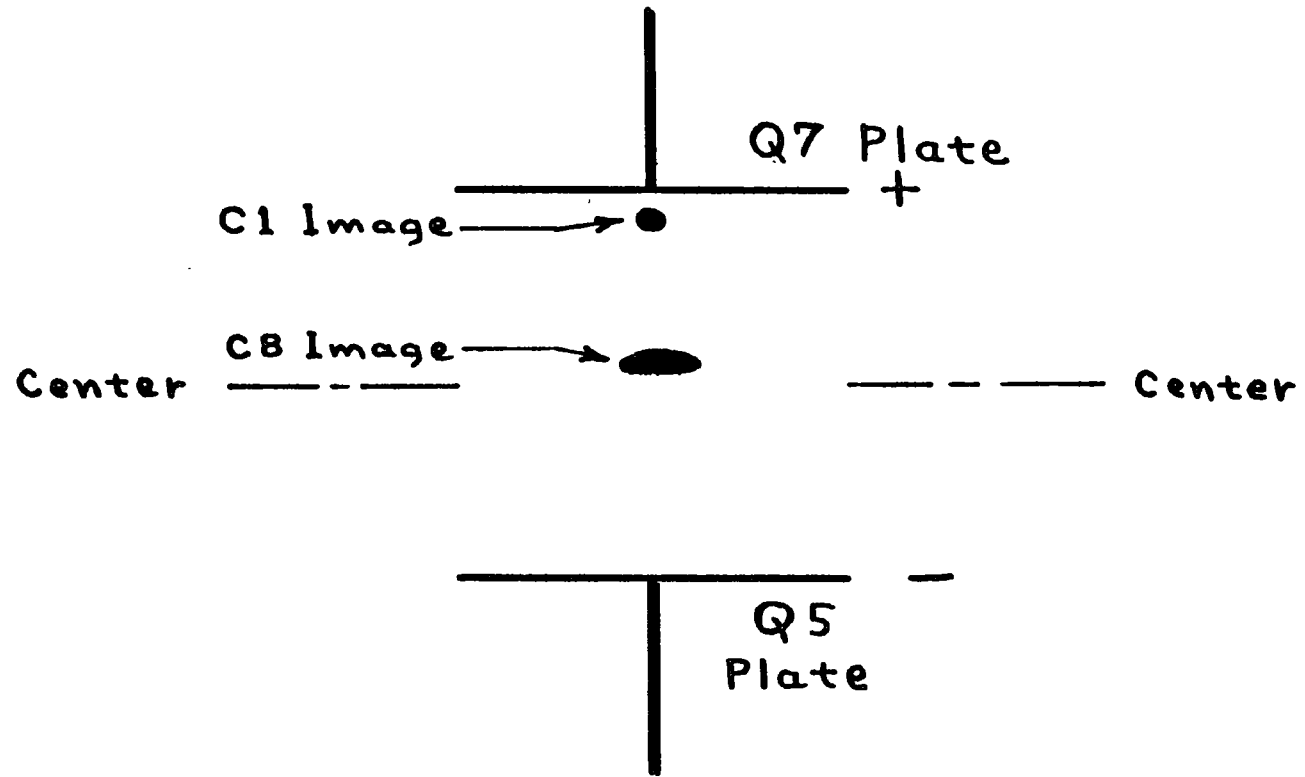
Each CST is slightly different, but the basic results are the same. With the same defect in the laboratory CST and the spacecraft CST, the intensity DN changes in the same direction as the CST cone angle position is changed from C3 to C8. In the laboratory CST the Δ DN is 2.8; in the spacecraft CST, the Δ DN is 5. This Δ DN is due to the defect in the CST which causes incorrect deflection voltages on the image dissector tube cone angle deflection plates and affects the electron-optical focusing inside the tube.

6.3 DEFOCUSING MECHANISM

The image dissector tube is designed so that, for proper electron focusing between the photocathode and the dissector aperture, the cone angle deflection plates must have the correct voltages. If not, the photo-electron image of the star, focused on the photocathode, will become defocused, and a large percentage of the photo-electrons will not pass through the narrow dissector aperture slit when they reach it. This is shown in Figure 13, Electron Beam Defocusing. When the CST is in cone-angle C1, the Q7 plate exercises most control of the photo-electron image and since the voltage on this plate is approximately correct, the photo-electron image is focused. As the cone angle commanded is moved towards the center of the field of view, plate Q5, with an incorrect voltage, is not contributing to the focusing of the photo-electron image. The image starts smearing, as shown, and a greater and greater percentage of the photo-electrons of which it is composed, do not go through the image dissector aperture slit, causing an apparent loss in intensity signal.

To ascertain the magnitude of this voltage unbalance across the deflection plates, the laboratory CST, with the simulated defect (resistor from base lead to ground) was commanded through all eight possible cone angles, and the voltages on the deflection plates were recorded. This is shown in Table 9, Voltages On Cone Angle Deflection Plates, shown on page 6-5.

6-4



ELECTRON BEAM DEFOCUSING

Figure 13. Electron Beam Defocusing

Table 9. VOLTAGE ON CONE ANGLE DEFLECTION PLATES

Normal Versus Defective Star Tracker

CONE ANGLE	NORMAL		DEFECTIVE		UNBALANCE VOLTS
	Q5 VOLTS	Q7 VOLTS	Q5 VOLTS	Q7 VOLTS	
C1	-54.3	+54.3	-54.3	+54.5	+ 0.1
C2	-28.8	+28.8	-28.6	+28.8	+ -0.2
C3	0	0	-27.9	+21.3	- 6.6
C4	+28.8	-28.8	-27.9	+16.2	-11.7
C5	+54.3	-54.3	-27.9	+10.6	-17.3
C6			-27.9	+ 5.4	-22.5
C7			-27.9	- 0.3	-28.2
C8			-27.9	- 5.6	-33.5

From Table 9, it is seen that in cone angle C8, the unbalance between the deflection plates is -33.5 volts. In a normally operating CST, the plus and minus voltages on the respective plates should be equal and balance out to zero. The increased unbalance voltage is causing the defocusing as the CST cone angles go from C1 to C8.

6.4 DEFOCUSING EFFECT ON DIM STARS

Also of concern is the effect of the deflection plate unbalance on stars dimmer than 1 x Canopus. After Saturn encounter, it is expected to guide on the star Vega, about one-half the brightness of Canopus. To verify how well the CST would perform on dimmer stars, the laboratory CST, with the simulated defect, was operated on the Canopus simulator. When in cone angles C2 and C3, intensity readings were taken for Canopus brightness from 1 x Canopus to less than 0.03 x Canopus. The same was done with the CST in cone angle C8. The results are shown in Figure 14, CST Intensity Readout For Dimmer Stars.

CST INTENSITY READOUT FOR DIMMER STARS

9-9

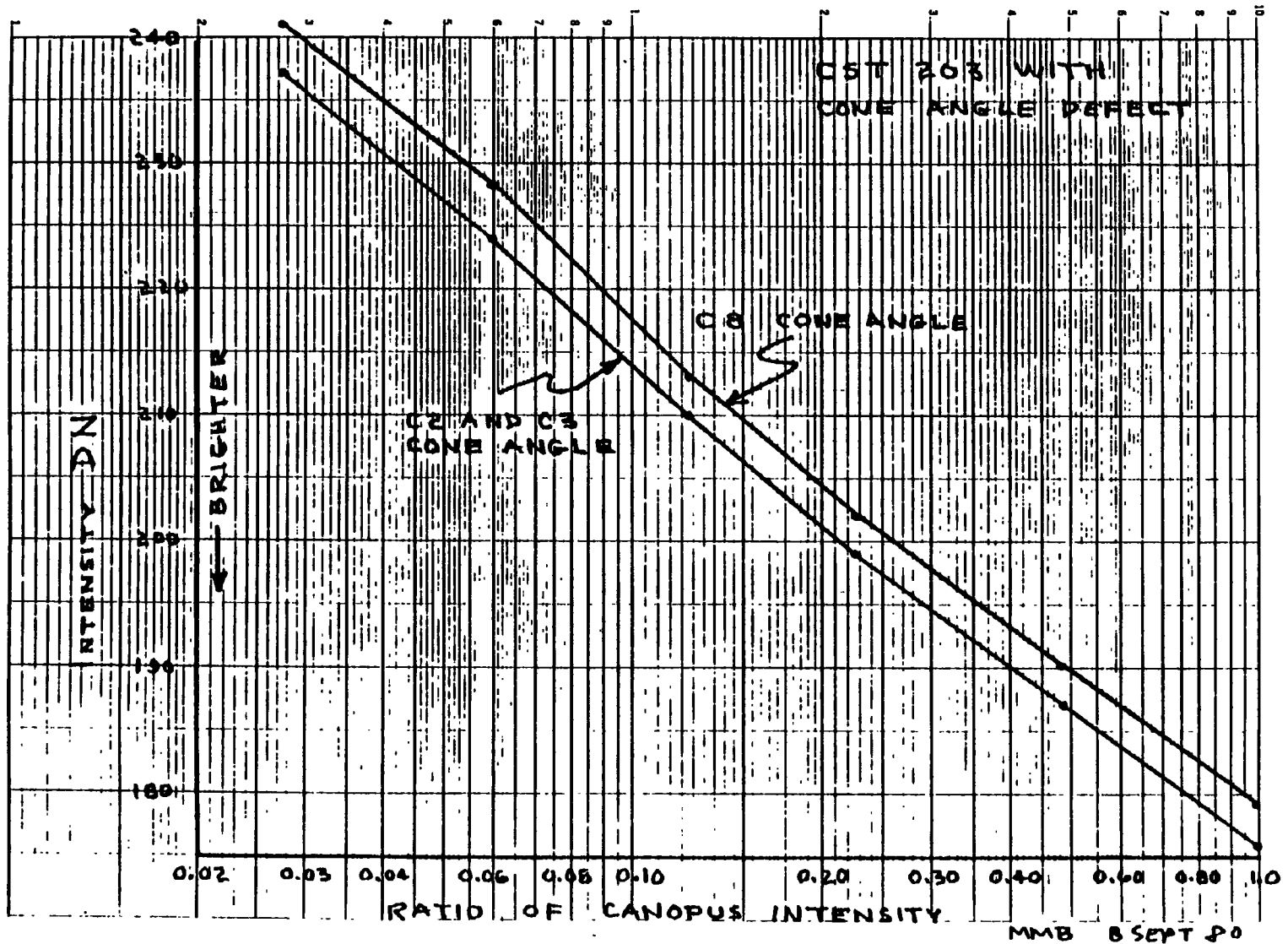


Figure 14. CST Intensity Readout For Dimmer Stars.

From the two curves on the Figure, it is seen that, no matter how bright or dim the star, the defocusing from cone angle C3 to C8 causes only a constant loss of approximately 3 to 4 DN's. The conclusion is that, even with the defect, the spacecraft CST can track Vega satisfactorily in cone angle C8.

6.5 DEFOCUSING EFFECT ON ROLL ERROR SIGNAL

A concurrent investigation was conducted on the effect of the defocusing on the CST roll error signal. Roll error signal noise was measured for various star intensities, first in cone angle C2, where there is hardly any defocusing; then in cone angle C8, where there is maximum defocusing. The results are shown in Figures 15 through 18. The results show that, though the roll error noise does increase as the defocusing increases, the roll error still remains within specification (3 arc-min. peak-to-peak) for star magnitudes greater than 0.06 x Canopus.

6.6 CONCLUSIONS

From the above investigation and data, the following conclusions can be made:

1. The CST photocathode has not lost sensitivity. The decrease of the intensity signal is due to defocusing of the photo-electron image because of incorrect voltages on the cone angle deflection plates.
2. The defocusing, at maximum, causes a change of approximately 3 to 4 DN regardless of real star intensity.
3. The roll error signal, though having more noise due to defocusing, still remains within specification for all guide stars which will be used.

To use the defective CST for Saturn encounter and beyond, operation in cone angle C4 is desired. Since the defective CST cannot go to cone angle C4, it must be operated in a cone angle which comes as close to C4 as possible. This turns out to be C8. When in C8, the CST will be able to sense Canopus through Saturn encounter, and Vega afterwards. Vega, however, will be within one degree from the edge of the field-of-view seen by cone angle C8. If nothing in the CST defective area changes, Vega will be sensed satisfactorily. The failure model described earlier, consisting of a carbonized path burned through the Delrin sleeve, or sleeves, as well as HF damage, has remained stable from April 1980 to the present. It is expected to remain unchanged, thus allowing the defective CST to complete the total Saturn encounter and the guiding to be done afterwards.

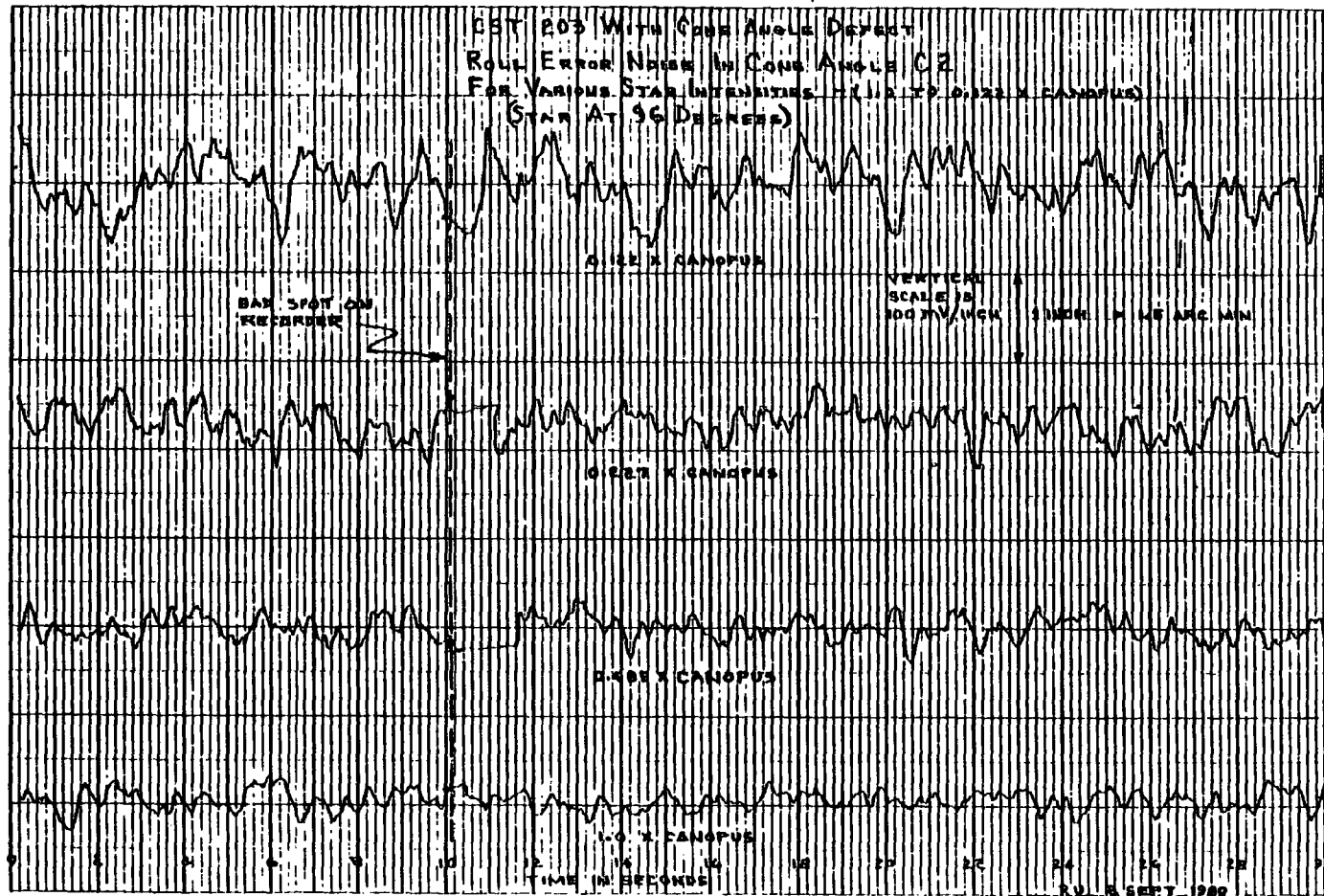


Figure 15. Roll Error Noise In Cone Angle C2 for Various Star Intensities (1.0 to 0.122 x Canopus)

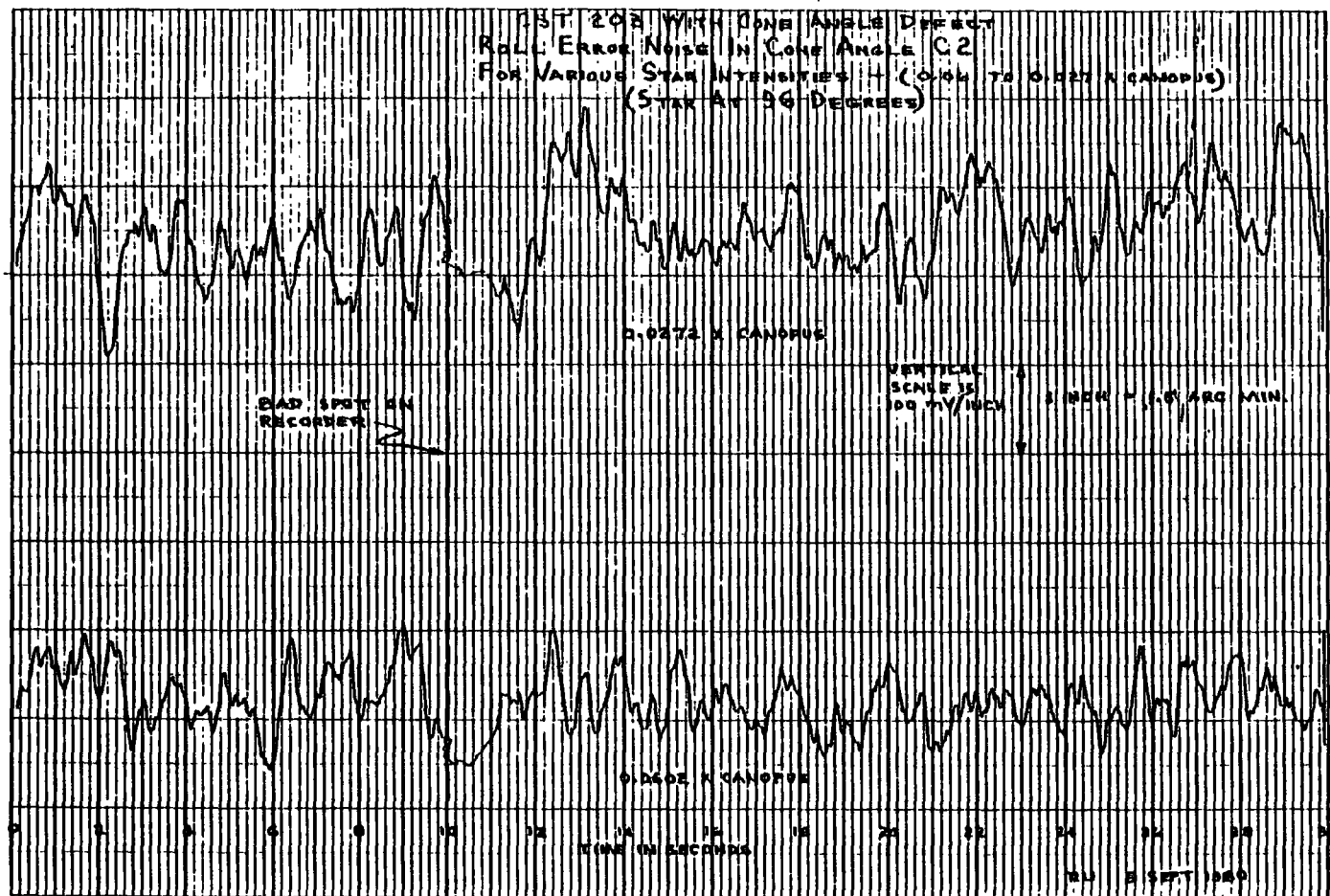


Figure 16. Roll Error Noise In Cone Angle C2 for Various Star Intensities (0.06 to 0.027 x Canopus)

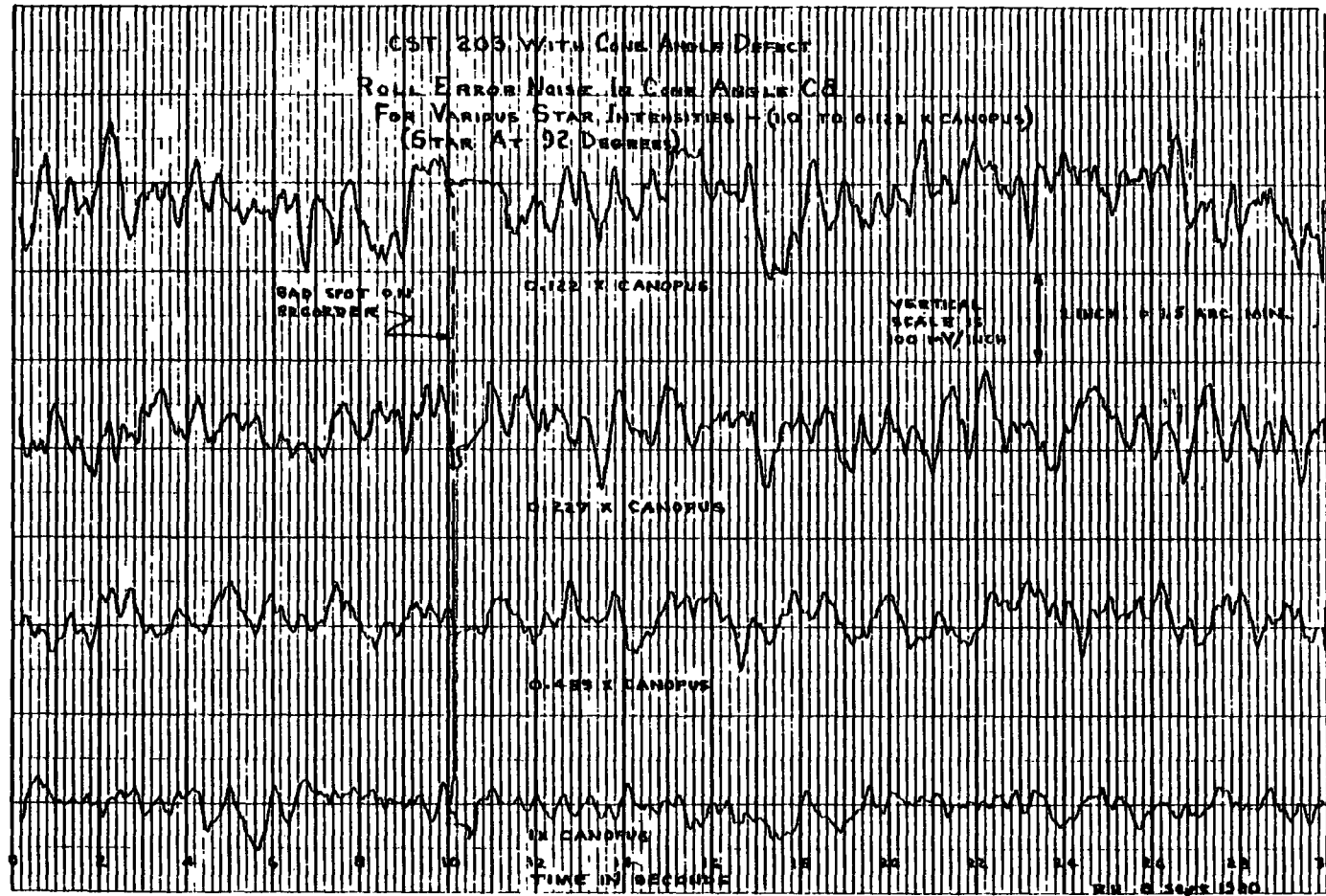


Figure 17. Roll Error Noise In Cone Angle C8 for Various Star Intensities
 (1.0 to 0.122 x Canopus)

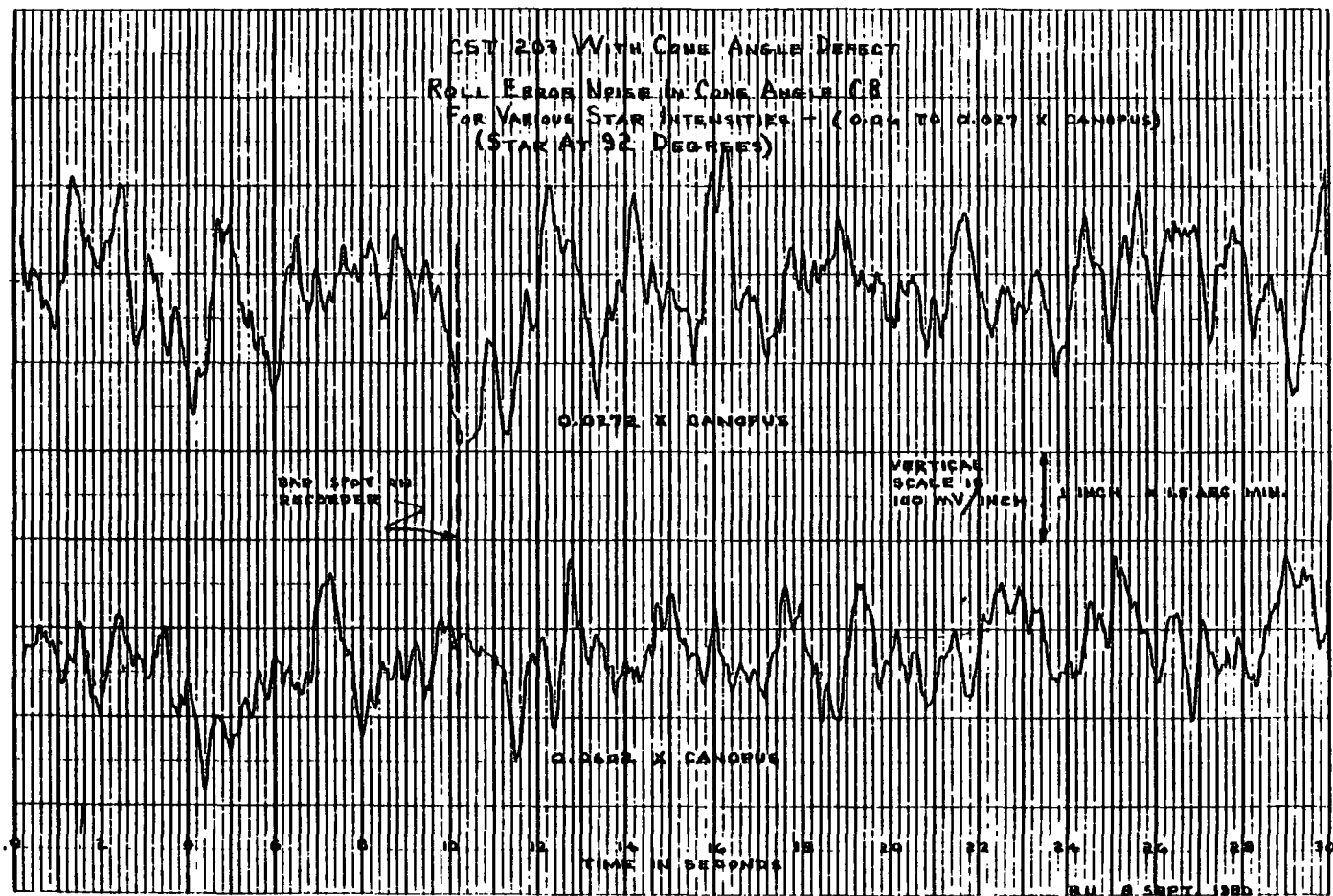


Figure 18. Roll Error Noise In Cone Angle C8 for Various Star Intensities (0.06 to 0.227 x Canopus)

APPENDIX A

ELECTROSTATIC CHARGING
OF THE
VOYAGER CANOPUS STAR TRACKER DELRIN AF SLEEVE
FOR THE CASE OF A FLOATING TUNGSTEN SPOT SHIELD

BY

Philip L. Leung

Section 357

ENVIRONMENTAL REQUIREMENTS, TEST, AND MECHANICAL SUPPORT

APPENDIX A

This report describes the results of an electro-static discharge (ESD) analysis on a Delrin AF sleeve in the Voyager Canopus Star Tracker. The Delrin AF sleeve is used to insulate Harris SDT 5553 transistor leads from a tungsten radiation spot shield which surrounds these transistors in the Voyager Canopus Star Tracker. The tungsten shield is glued to the ground plane through a layer of epoxy, as shown in Figure A-1, Schematic Of Tungsten Spot Shield. The shield is not grounded and is floating. The thickness of the epoxy layer is about 50 mils, although the exact value is unknown. In the case of a floating tungsten shield, there are two major concerns:

1. The current through the base lead of the transistor may be large enough to cause damage to the transistor.
2. The peak electric field inside the Delrin AF may exceed the breakdown value.

Because of the complexity of the physical configuration, a macroscopic approach is used. The actual physical configuration, shown in Figure A-1, is represented by an equivalent circuit, as shown in Figure A-2, Equivalent Circuit of Figure A-1. Using standard techniques in circuit analysis, the important currents and potentials are determined.

In the equivalent circuit shown in Fig. A-2, the source current, I_s , is the electron current available for the charging of the Delrin. Since the tungsten spot shield is very massive and has large surface areas, the source current is essentially the electron current deposited inside the tungsten shield. The current deposited directly in the Delrin is very small compared to that deposited in the tungsten spot shielding (see later analysis) and is neglected. As a worst case analysis, it is assumed that the density of deposited current in the tungsten shield, (J_d), is the same as the current density of electrons that penetrate the mass shielding (J_p).

Table A-1 shows the integral peak electron flux, (J_p), for the July 1978 and February 1979 Jupiter radiation models, and for two different values of mass shielding. In the determination of the source current, the highest value of integral peak electron flux is used; this value of 8.05×10^7 e/cm²-s corresponds to the February 1979 model with 0.5 gm/cm² of mass shielding. For this case, a source current of 7.4×10^{-11} amp is obtained (details are presented in note 1).

The resistivity of Delrin is given in Table A-2. Its value ranges from 5×10^{14} to 10^{15} ohm-cm. However, the resistivity for the particular Delrin used on the star tracker, Delrin AF, is not given. In this appendix, analyses are performed with resistivity values of 10^{15} ohm-cm and 10^{14} ohm-cm. The lower the resistivity of Delrin, the higher the current that will flow through the base of the SDT 5553 transistor. Thus, resistivity of 10^{14} ohm-cm for Delrin gives a worst case result as far as the base current of the SDT 5553 transistor is concerned. A resistivity of 10^{15} ohm-cm is also used because it gives the worst case result, as far as the breakdown electric field is concerned. The calculation of the equivalent resistance of the Delrin sleeve (R_d) is shown in Note 2.

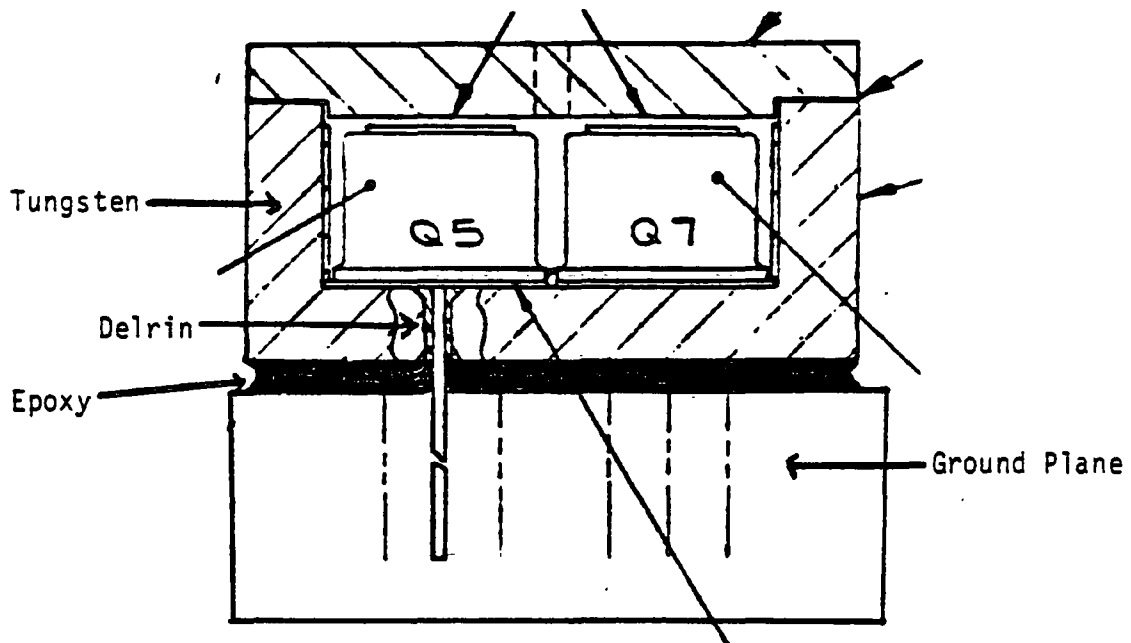
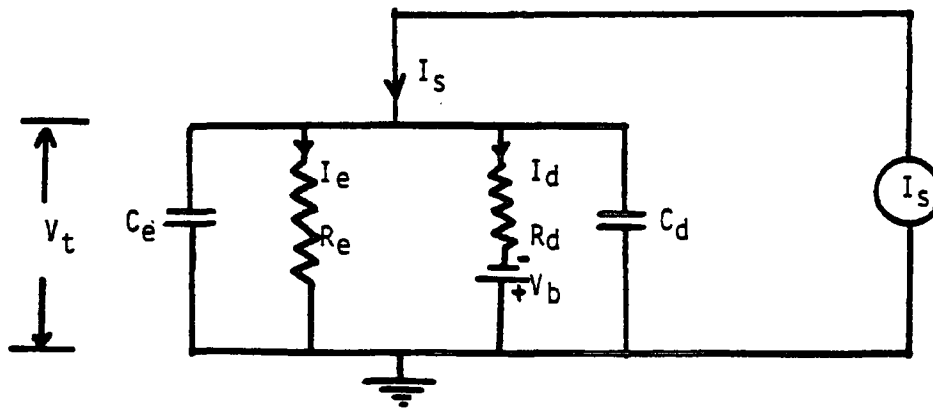


Figure A-1. Schematic of the tungsten spot shield



- I_s = Source current
- R_d = Resistance of Delrin sleeve
- C_d = Capacitance of Delrin sleeve
- R_e = Resistance of the epoxy layer
- C_e = Capacitance of the epoxy layer
- I_d = Current through the base of the 5553 transistor
- I_e = Current through the epoxy layer
- V_t = Voltage of the tungsten spot shield
- V_b = Bias of the base of 5553 transistor with respect to ground = 75 volt

Figure A-2. Equivalent circuit of Figure A-1.

TABLE A-1.

VOYAGER 1 JUPITER ENCOUNTER PEAK ELECTRON FLUX SPECTRA

ENERGY INTERVAL		INTEGRAL PEAK ELECTRON FLUX 1.5 g/cm ² , 2/79 Md1	INTEGRAL PEAK ELECTRON FLUX 1.5 g/cm ² , 7/78 Md1	INTEGRAL PEAK ELECTRON FLUX 0.5 g/cm ² , 2/79 Md1	INTEGRAL PEAK ELECTRON FLUX 0.5 g/cm ² , 7/78 Md1
E _{max} (Mev)	E _{min} (Mev)	(e/cm ² -s)	(e/cm ² -s)	(e/cm ² -s)	(e/cm ² -s)
100	25.1	3.72(+6)	3.79(+5)	4.93(+6)	5.11(+5)
25.1	20.0	6.70(+6)	6.88(+5)	8.77(+6)	8.70(+5)
20.0	15.8	1.08(+7)	1.05(+6)	1.44(+7)	1.36(+6)
15.8	12.6	1.64(+7)	1.54(+6)	1.97(+7)	1.82(+6)
12.6	10.0	3.08(+7)	1.91(+6)	2.60(+7)	2.35(+6)
10.0	7.94	3.61(+7)	2.37(+6)	3.11(+7)	2.72(+6)
7.94	6.31	3.06(+7)	2.72(+6)	3.57(+7)	3.01(+6)
6.31	5.01	3.39(+7)	2.93(+6)	4.05(+7)	3.25(+6)
5.01	3.98	3.75(+7)	3.15(+6)	4.47(+7)	3.40(+6)
3.98	3.16	4.04(+7)	3.31(+6)	4.93(+7)	3.57(+6)
3.16	2.51	4.28(+7)	3.42(+6)	5.39(+7)	4.95(+6)
2.51	2.00	2.47(+7)	3.50(+6)	5.84(+7)	6.78(+6)
2.00	1.58	4.63(+7)	3.58(+6)	6.27(+7)	9.13(+6)
1.58	1.26	4.77(+7)	3.66(+6)	6.68(+7)	1.32(+7)
1.26	1.00	4.87(+7)	3.79(+6)	6.97(+7)	1.64(+7)
1.00	7.94(-1)	4.95(+7)	3.87(+6)	7.25(+7)	2.06(+7)
7.94(-1)	6.31(-1)	5.02(+7)	3.94(+6)	7.44(+7)	2.27(+7)
6.31(-1)	5.01(-1)	5.07(+7)	4.01(+6)	7.63(+7)	2.52(+7)
5.01(-1)	3.98(-1)	5.10(+7)	4.05(+6)	7.74(+7)	2.65(+7)
3.98(-1)	3.16(-1)	5.14(+7)	4.10(+6)	7.84(+7)	2.77(+7)
3.16(-1)	2.51(-1)	5.16(+7)	4.13(+6)	7.92(+7)	2.87(+7)
2.51(-1)	2.00(-1)	5.17(+7)	4.15(+6)	7.97(+7)	2.93(+7)
2.00(-1)	1.58(-1)	5.18(+7)	4.16(+6)	8.01(+7)	2.98(+7)
1.58(-1)	1.26(-1)	5.19(+7)	4.16(+6)	8.03(+7)	3.01(+7)
1.26(-1)	1.00(-1)	5.19(+7)	4.17(+6)	8.05(+7)	3.03(+7)

NOTE: 3.72(+6) IS EQUIVALENT TO 3.72 x 10⁶

YTEL nylon resins

612 NYLONS					
YTEL 500	YTEL 500 COMBUSTION TO 99% RES	YTEL 500	YTEL 500 COMBUSTION TO 99% RES	YTEL 500	YTEL 500 COMBUSTION TO 99% RES
13,500(-40°F)	11,500(-40°F)	11,500(-40°F)	11,500(-40°F)	11,500(-40°F)	11,500(-40°F)
8,000	7,500	8,000	8,000	8,000	8,000
5,900(170°F)	-	5,900(170°F)	-	5,900(170°F)	-
10(-40°F)	20(-40°F)	15(-40°F)	30(-40°F)	15(-40°F)	30(-40°F)
100	250	150	300	150	300
-	-	-	-	-	-
250,000	100,000	250,000	100,000	250,000	100,000
8,400	-	8,600	-	8,600	-
0.65	0.46	0.6	0.6	0.9	0.60
0.05	1.20	1.0	1.4	1.00	1.40
-	-	-	-	-	-
-	-	-	-	-	-
-	-	2,400	-	2,400	-
0114	-	0114	-	0114	-
1.6	-	1.6	-	1.6	-
5x10 ⁻³	-	5x10 ⁻³	-	5x10 ⁻³	-
1.5	-	1.5	-	1.5	-
0.3-0.5	-	0.3-0.5	-	0.3-0.5	-
100(10)	-	100(10)	-	100(10)	-
130(10)	-	130(10)	-	130(10)	-
-	Dielectric Strength				
5x10 ¹³	10 ¹⁴	10 ¹⁴	10 ¹⁴	5x10 ¹³	10 ¹⁴
-	Volume Resistivity				
-	Arc Resistance				
4.0	5.3	3.3	5.0	4.0	5.3
3.5	4.0	3.0	3.2	3.5	4.0
-	-	-	-	-	-
0.02	0.04	0.02	-	0.02	0.04
0.02	0.03	0.02	-	0.02	0.03
-	-	-	-	-	-
-	-	-	-	-	-
0.4	-	0.4	-	0.4	-
3.0	-	3.0	-	3.0	-
-	-	-	-	-	-
-	Self-exting				
1.06-1.08	-	1.06-1.08	-	1.06-1.08	-
0.011	-	0.011	-	0.011	-
-	-	-	-	-	-

DELTRIN acetal resins					L	
DELTRIN 100 SERIES	DELTRIN 200 SERIES	DELTRIN 300 SERIES	DELTRIN 570 SERIES	DELTRIN 67	LICITE 30 100	LICITE 20 100
14,700	14,700	14,700	13,700	9,000	14.5x10 ³	14.5x10 ³
10,000	10,000	10,000	8,500	6,900	9.5x10 ³	10.0x10 ³
7,500	7,500	7,500	5,500	4,700	>3.5x10 ³	>4.0x10 ³
30	13	11	5	6	2	2
75	25	15	7	12	3-5	3-5
>250	>250	>250	16	30	100	90
410,000	410,000	410,000	880,000	400,000	1.5-4.5x10 ⁵	6-9x10 ⁵
9,500	9,500	9,500	9,500	8,000	7.5x10 ⁴	9.0x10 ⁴
1.8	1.2	1.0	0.5	0.6	-	-
2.3	1.4	1.3	0.8	0.7	0.3	0.3
-	-	-	-	-	3.4x10 ³	4.1x10 ³
14,100	14,100	14,100	-	-	1.5x10 ⁴	1.5x10 ⁴
5,200	5,200	5,200	5,200	4,500	-	-
M94, R120	M94, R120	M94, R120	M90, R110	M78, R110	M85	M90
0.5	0.5	0.5	0.5	-	-	0.7
300	300	300	-	-	-	-
4.2x10 ⁻³ (-40° to +85°F)	4.2x10 ⁻³ (-40° to +85°F)	4.2x10 ⁻³ (-40° to +85°F)	2.0-4.5x10 ⁻³ (-40° to +85°F)	4.5x10 ⁻³ (-40° to +85°F)	6x10 ⁻⁴	4x10 ⁻⁴
1.6	1.6	1.6	-	-	1.4	1.4
0.35	0.35	0.35	-	-	0.35	0.35
255	255	255	315	212	166	180
338	338	338	365	220	175	180
Excellent	Excellent	Excellent	Excellent	Excellent	Excellent	Excellent
1x10 ¹³	1x10 ¹³	1x10 ¹³	5x10 ¹⁴	-	10 ¹⁴	10 ¹⁴
120cm	120cm	120cm	100	-	No tracking	No tracking
3.7	3.7	3.7	4.0	-	3.0	3.0
3.7	3.7	3.7	4.0	-	3.6	3.4
3.7	3.7	3.7	3.9	-	2.9	2.9
0.003	0.003	0.003	0.004	-	0.04	0.04
0.003	0.003	0.003	0.004	-	0.04	0.04
0.005	0.005	0.005	0.005	-	0.03	0.03
-	-	-	-	-	1.491	1.491
-	-	-	-	-	92	92
-	-	-	-	-	<3	<3
0.25	0.25	0.25	0.25	0.20	0.3	0.3
0.9	0.9	0.9	1.0	-	-	-
-	-	-	-	-	<0.1	<0.1
1.1	1.1	1.1	0.9	0.8	0.8-1.2cm	0.8-1.2cm
1.42cm	1.42cm	1.42cm	1.36	1.54	1.18	1.18
0.015-0.030	0.015-0.030	0.015-0.030	0.01-0.02cm	0.015-0.030cm	0.002-0.005	0.002-0.007
Return	Return	Return	-	-	Excellent	Excellent

Table A-2. Properties of Delrin

The layer of epoxy between the tungsten spot shield and the printed circuit board forms a bulk resistor between two parallel conducting plates. Since the exact thickness of the epoxy layer (t) is unknown, it is a variable in the analysis. The equivalent resistance of the epoxy layer (R_e) changes as the thickness changes (calculation of R_e is shown in Note 3). The resulting base current and the peak electric field inside the Delrin are then determined as a function of R_e . In order to perform the circuit analysis, Kirchoff's law and the macroscopic Ohm's law are applied. From Fig. A-2, and using Kirchoff's law:

$$I_s = I_e + I_d \quad (1)$$

The condition given by eq (1) states that, at steady state, the deposited current (I_s in this case) is equal to the leakage current ($I_e + I_d$).

The potential of the tungsten shield (V_t) is given by:

$$V_t = I_e R_e = I_d R_d - 75 \quad (2)$$

Substituting eq. (2) in eq. (1):

$$I_s = (I_d R_d - 75) / R_e + I_d$$

$$I_d = \frac{I_s + 75 / R_e}{1 + R_d / R_e} \quad (3)$$

A maximum of 75 volts is on the transistor collector and emitter leads.

From equation (3) I_d , which is the current through the base of the SDT 5553 transistor, can be determined. The voltage of the tungsten spot shield (V_t) is then determined from equation (2). Once V_t is known, the peak electric field (E_p) inside the Delrin can be determined (see Note 4). Table A-3a and A-3b tabulate the value of I_d , V_d , and E_p for various values of thickness of epoxy. Table A-3a is for a resistivity of Delrin equal to 10^{14} ohm-cm, and Table A-3b is for a resistivity of Delrin equal to 10^{15} ohm-cm.

From these Tables, it is observed that the base current of the transistor is always less than 1 nanoamp, and the peak electric field is always less than the breakdown electric field value of 1700 V/mil. Consequently the electrostatic charging of the Delrin sleeve by the Jupiter encounter charging mechanism alone does not cause any significant problem.

In this Appendix, worst case analyses are presented. In these analyses, the current density of the deposited current (J_d) is assumed to be equal to the current density of electrons that penetrate the mass shielding (J_p). In the actual case, J_d is only a fraction of J_p . Detailed calculations of the charging current are presented in Note 5. In this Note, it is shown that the density of deposited current, J_d , in the case of a floating tungsten shield, is 75% of J_p . Consequently for a floating tungsten shield, actual values of electric field are very close to the worst case values presented in this appendix.

TABLE A-3
RESULTS OF CIRCUIT ANALYSIS

Table A-3a

$$\eta = 10^{14} \text{ Ohm-cm}, R_d = 2.9 \times 10^{13} \text{ Ohm}$$

t(mil)	$R_e(\Omega)$	$I_d(\text{Amp})$	$V_t(\text{volt})$	$E_p(\text{V/mil})$
5	2.9(11)	3.3(-12)	21	2.9
10	5.8(11)	4.0(-12)	41	5.7
25	1.5(12)	6.0(-12)	99	14
50	2.9(12)	9.1(-12)	190	26
100	5.8(12)	1.5(-11)	350	48

Table A-3b

$$\eta = 10^{15} \text{ Ohm-cm}, R_d = 2.9 \times 10^{14} \text{ Ohm}$$

t(mil)	$R_e(\Omega)$	$I_d(\text{Amp})$	$V_t(\text{volt})$	$E_p(\text{V/mil})$
5	2.9(11)	3.3(-13)	21	3.0
10	5.8(11)	4.1(-13)	43	6.0
25	1.5(12)	6.3(-13)	110	15
50	2.9(12)	9.9(-13)	210	30
100	5.8(12)	1.7(-12)	420	59

NOTE: Breakdown electric field of Delrin is 1700 V/mil

The layer of epoxy (Fig. A-1) plays a very important role in the analyses presented in this Appendix. Because of the relatively low resistivity of epoxy (10^{14} Ohm-cm), this layer provides a low leakage resistor (R_e in Fig. A-2) for the charging current, thus reducing the charging current to the Delrin. In the absence of the layer of epoxy, the internal electric field of the Delrin can be much higher than that presented in Table A-2.

Although the electrostatic breakdown of unflawed Delrin is unlikely in the Canopus Star Tracker, the floating tungsten spot shield does cause the shield to charge up to high potential values (~ 300 Volt), creating a large electric field inside the Delrin. If the Delrin is flawed by microvoids or scratches, the effective contact area will be greatly reduced. This will increase the equivalent resistance of the Delrin sleeve (R_d) and the resulting voltage on the tungsten shield will then be higher. This higher voltage, coupled with the reduction in thickness of the Delrin in some part of the sleeve, may cause electrical breakdown through the "defective area" of the sleeve.

NOTE 1

Calculation of the Source Current

Figures A-3 and A-4 show the dimensions of the tungsten spot shield. The following computations are for the surface areas of the tungsten shield.

$$\text{Area of the top cover} = (1.105 \times .680 - 4 \times \frac{.188 \times 188}{2}) = 0.68 \text{ sq. in.}$$

$$\text{Area of section A-A} = (.465 + .150) \times .680 = 0.42 \text{ sq. in.}$$

$$\text{Area of the side wall perpendicular to A-A} = 1.105 \times (.465 + .150) = 0.68 \text{ sq. in.}$$

$$\text{Total surface area A} = (0.68 + 0.42 + 0.68) \times 2 \text{ sq. in.} = 22.9 \text{ sq. cm.}$$

The total source current, I_s , is given by:

$$I_s = 1/4 J_p e$$

where:

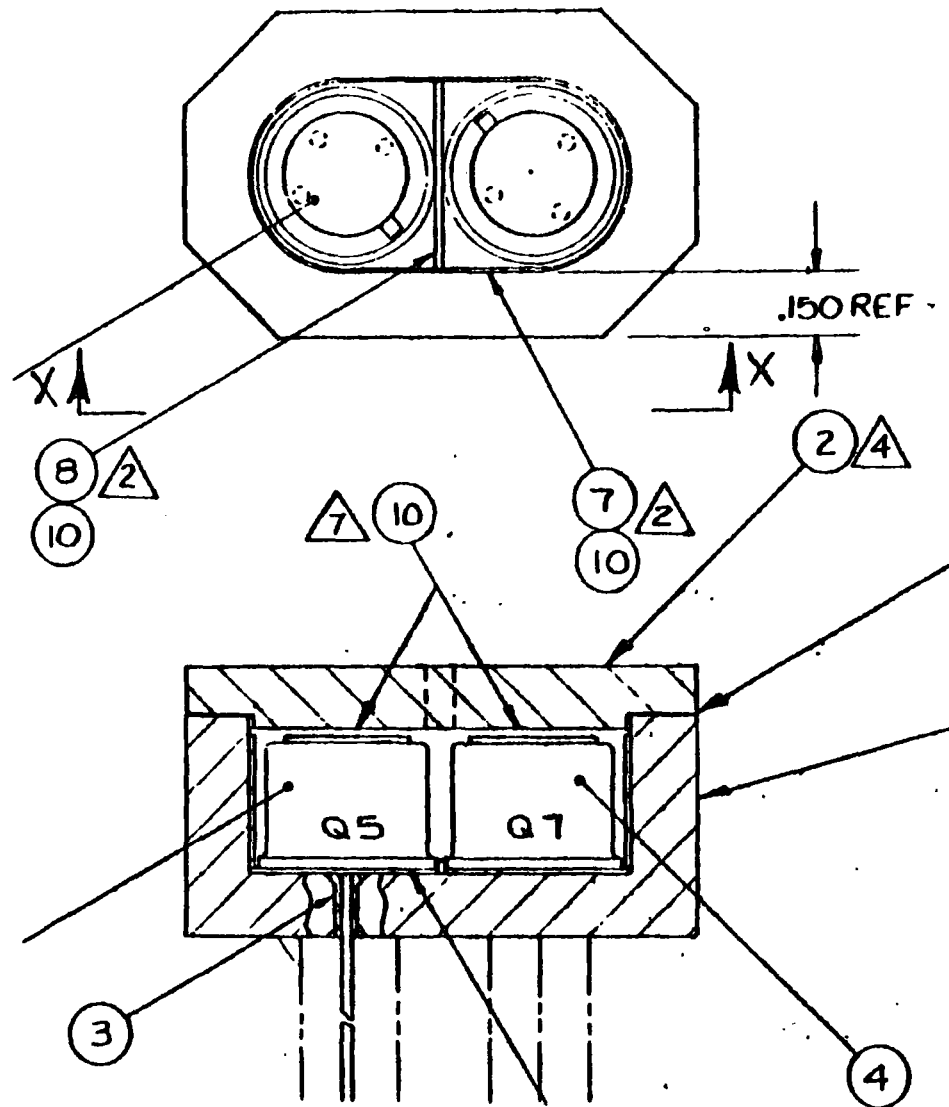
A = total surface area

e = electron charge = 1.6×10^{-19} coulomb

J_p = omnidirectional particle flux that penetrates the mass shielding
= 8.05×10^7 e/cm²-sec (worst case value)

The factor 1/4 in determination of I_s , is composed of two factors of 1/2. The first accounts for the fact that only half of the particles coming towards the surface are collected. The second factor of 1/2 is merely the average of directional cosine over the surface area (reference 1).

$$\begin{aligned} I_s &= 1/4 \times 8.05 \times 10^7 \times 22.9 \times 1.6 \times 10^{-19} \\ &= 7.4 \times 10^{-11} \text{ A/cm}^2 \end{aligned}$$



SDT 5553 TRANSISTORS ASSEMBLED IN CONTAINER

Figure A-3. SDT 5553 Transistors Assembled In Container

A-11

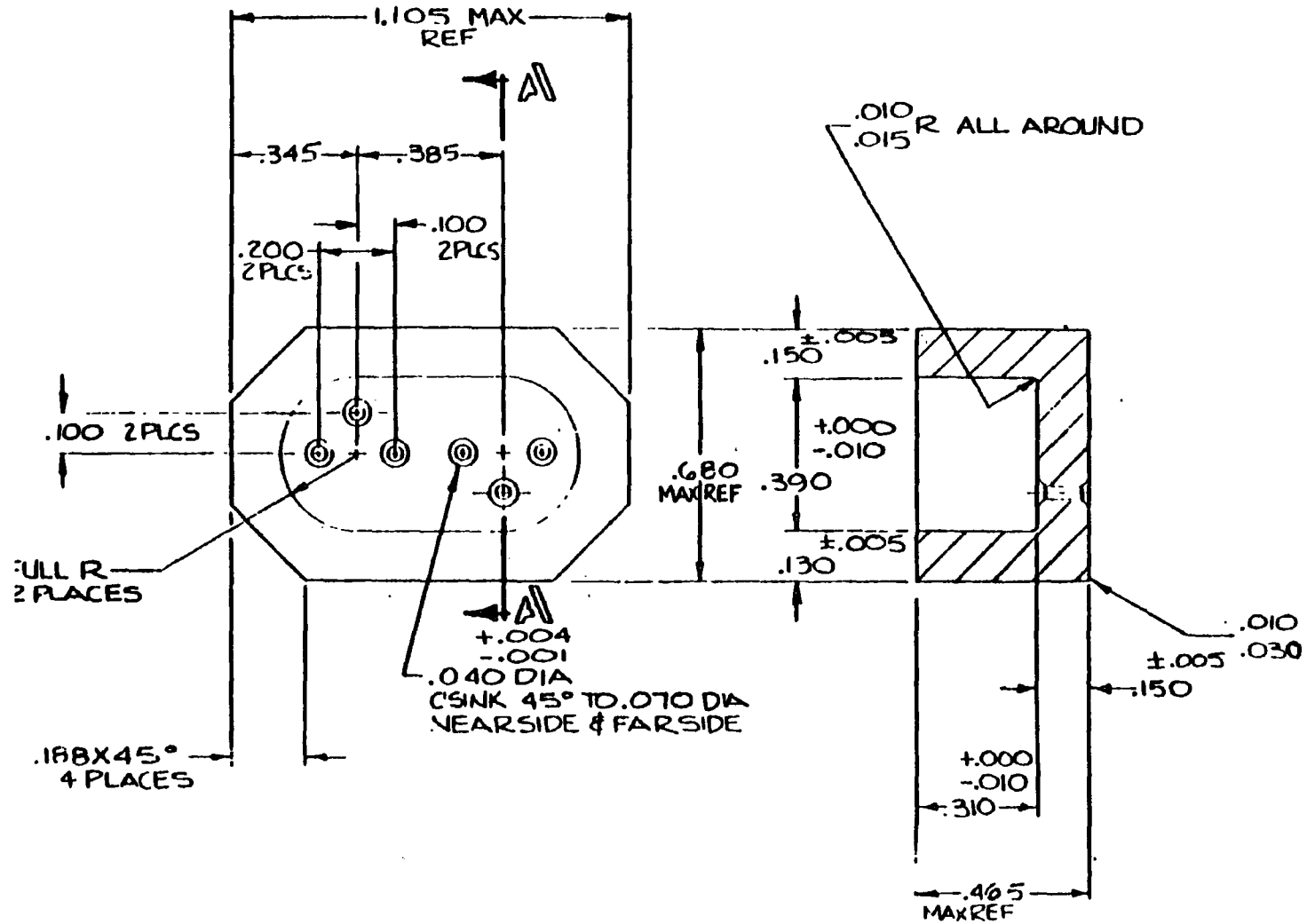


Figure A-4. Tungsten Spot Shield Box

NOTE 2

Calculation of the Resistance of a Delrin Sleeve

The physical configuration of this resistor can be represented by a coaxial line (Fig. A-5). The base lead of the SDT 5553 transistor forms the center conductor, the tungsten shielding forms the outer conductor, and the Delrin AF forms the insulator between the conductors.

The direction of current flow in this resistor is indicated by the arrow in Fig. A-5. The value of resistance of the Delrin sleeve, R_d , is derived below.

$$dR(r) = \frac{\eta dr}{2\pi r \ell} \left[\text{Resistance} = \frac{\text{resistivity} \times \text{length}}{\text{Area}} \right]$$

$$\begin{aligned} R_d &= \int_{a_1}^{a_2} dR(r) = \int_{a_1}^{a_2} \frac{\eta dr}{2\pi r \ell} \\ &= \frac{\eta}{2\pi \ell} \ln \frac{a_2}{a_1} \end{aligned}$$

where:

ℓ = length of Delrin sleeve = 0.150"

a_1 = radius of the transistor lead = 0.010"

a_2 = radius of the Delrin sleeve = 0.020"

η = resistivity of Delrin AF

for: $\eta = 10^{15}$ ohm-cm

$R_d = 2.9 \times 10^{14}$ ohm

for: $\eta = 10^{14}$ ohm-cm

$R_d = 2.9 \times 10^{13}$ ohm

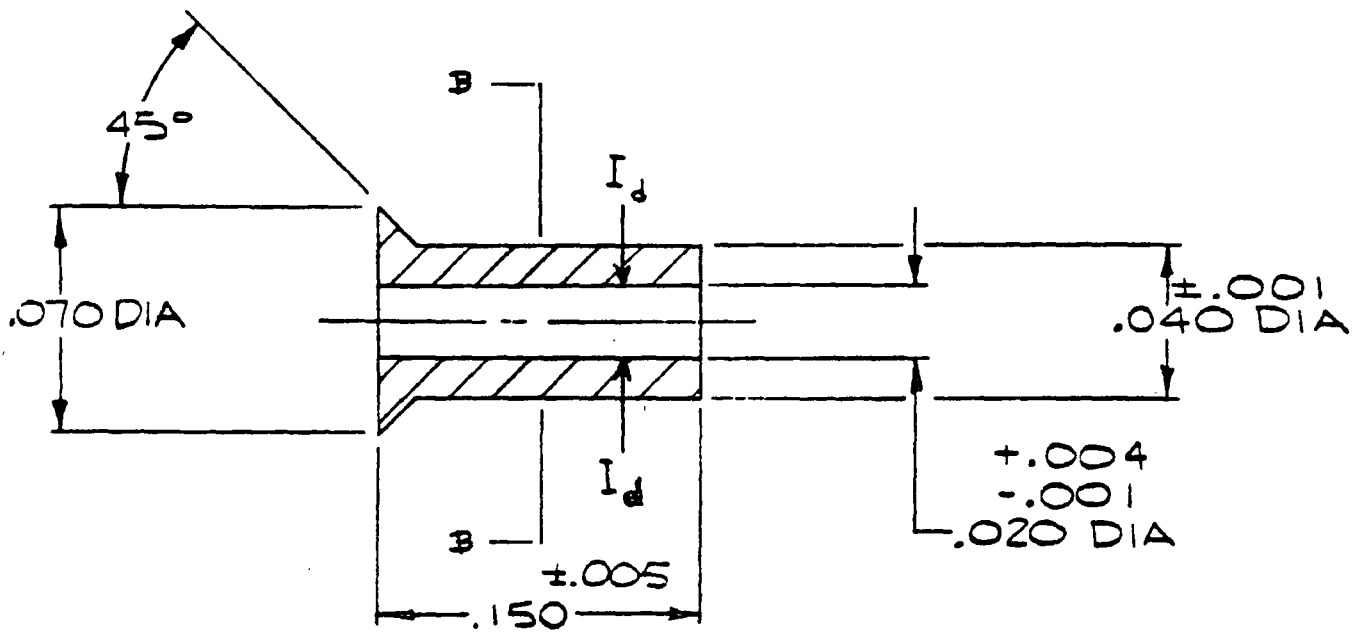


Figure A-5. Delrin Sleeve

NOTE 3

Resistance of the Epoxy Layer

The epoxy fills the space between the tungsten shielding and the ground plane. It can be represented by a bulk resistor between two parallel plates. The resistance is:

$$R_e = \frac{\eta_e t}{A}$$

$$\eta_e = \text{Resistivity of epoxy} = 10^{14} \text{ ohm-cm}$$

$$A = \text{Surface area of epoxy} = (1.105 \times .680 - 4 \times .188 \times .188/2) = .68 \text{ sq. in.}$$

$$t = \text{Thickness of epoxy layer}$$

$$R_e = \frac{10^{14} \times t(\text{mil}) \times 2.54}{.68 \times 2.54 \times 2.54 \times 1000} = 5.8 \times 10^{10} \times t(\text{mils}) \text{ ohm}$$

NOTE 4

Electric Field of Delrin Sleeve

The electric field of a coaxial line is given by the following formula (Reference 2):

$$E(r) = \frac{V}{r \ln \frac{a_2}{a_1}}$$

where: V = potential difference between the inner and outer conductor

r = radial position

The peak electric field inside the Delrin is:

$$E_p = \frac{V}{a_1 \ln \frac{a_2}{a_1}} = 0.14 (V_t - 75) \text{ Volts/mil}$$

Calculation of Charging Current for Delrin

In this configuration, the main source of charging current is the current deposited in the tungsten spot shield.

$$\text{Density of tungsten} = 19.3 \text{ gm/cm}^3$$

$$\text{Area of the tungsten shield} = 22.9 \text{ cm}^2$$

$$\text{Thickness of tungsten shield} = .150" = .38 \text{ cm}$$

$$\text{Stopping power} = \rho t = 7.35 \times 10^3 \text{ mg/cm}^2$$

From Fig. A-6, electrons with $E < 13 \text{ MeV}$ are stopped inside the tungsten; consequently, the deposited current is:

$$\begin{aligned} J_d &= J(0) - J(13 \text{ MeV}) = 8.05 \times 10^7 - 1.97 \times 10^7 \text{ /cm}^2\text{-s} \\ &= 6.08 \times 10^7 \text{ /cm}^2\text{-s} \end{aligned}$$

$$\frac{J_d}{J_p} = 75\%$$

$$\begin{aligned} \text{Total current deposited} &= J_d \times A \times e/4 \\ &= 5.5 \times 10^{-11} \text{ Amp} \end{aligned}$$

For the case of a floating spot shield, part of the current that is deposited in the shield flows through the Delrin, and the other part flows through the layer of epoxy. From Table A-3b, and for $t = 25 \text{ mils}$, the charging current (I_d) of Delrin is:

$$I_d = 6.3 \times 10^{-13} \text{ Amp}$$

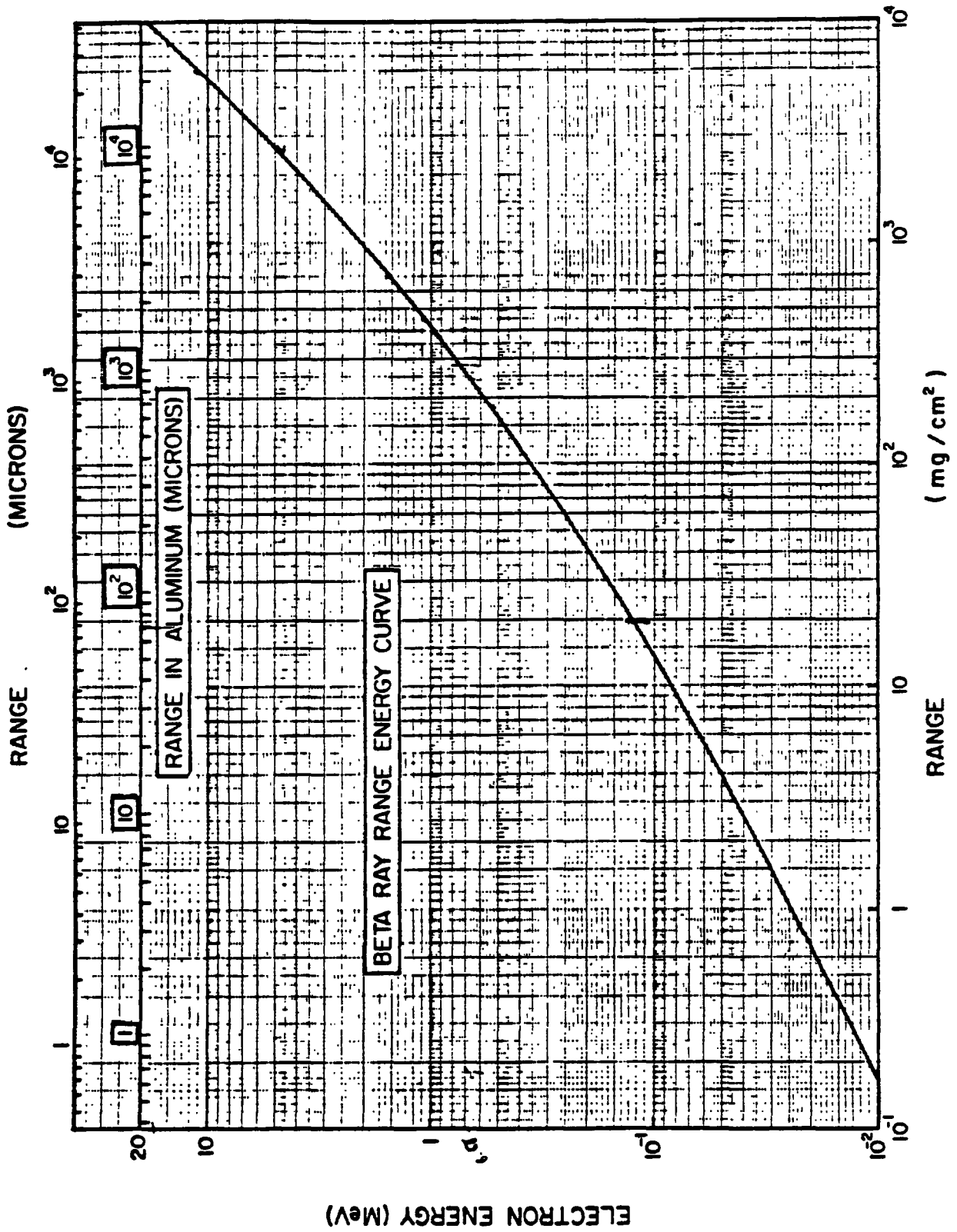


Figure A-6. Range Curve

REFERENCES FOR APPENDIX

1. Plasma Diagnostic Techniques, Huddleston and Leonard, Academic Press, 1965.
2. Reference Data for Radio Engineers, Howard W. Sams and Co., Inc.